NTNU

Norwegian University of
Science and Technology

Viability study of Acoustic Emission for condition monitoring of coiled tubing

Christoffer Torkildsen Stenerud

Subsea Technology
Submission date: June 2017
Supervisor: Olav Egeland, MTP

Norwegian University of Science and Technology
Department of Mechanical and Industrial Engineering

PREFACE

First, I would like to thank my supervisors Associate Professor Ragnar Gjengedal and Professor Olav Egeland for their academic guidance, valuable input, encouragement and assistance from preparation to completion of this thesis.

Second, I would like to express my appreciation to the bachelor group consisting of; Morten Ståløy, Anders Kjellevoll, Alexander Næsheim and Mads Nåmdal for their dedicated work ethic and excellent performance on acquiring the necessary equipment and setting up the laboratory for the acoustic emission tests. I would also like to thank ClampOn for providing the transducer, software and for their technical support throughout the experimental phase of this thesis.

Finally yet importantly, I would like to thank my family and girlfriend for their unending support and motivation throughout the period of my master's studies.

Christoffer Torkildsen Stenerud

Bergen, June 2017

SAMMENDRAG

Akustisk emisjon refererer til utstråling av elastiske bølger som blant annet genereres av sprekkvekst eller andre skadelige prosesser i et material. Innspilling og analyse av disse bølgene danner grunnlaget til monitoreringsteknikken Akustisk Emisjon (AE). Metoden brukes innenfor områder som materiell forskning samt inspeksjon og monitorering av strukturer. Videre er monitorering av initiering og vekst av utmattelsessprekker, et område hvor metoden har vist mye potensiale både i teori og praksis.

Gjennom et omfattende litteratursøk, evaluerer denne avhandlingen akustisk emisjons egnethet til monitorering av kveilerør. Ved å studere de mest fremtredende feilmodi for kveilerør samt eksisterende teknologi og metoder for inspeksjon av kveilerør, belyses behovet for utmattelsesmonitorering. Deretter presenteres de potensielle fordelene og utfordringene ved å anvende akustisk emisjon til dette formålet, samt en foreslått løsning på hvordan det kan gjennomføres.

Videre ble det gjennomført både strekk og utmattelsestester av lavkarbonstål hvor akustisk emisjon ble brukt til monitorering av materialets skadeutvikling. Utstyret var et rekonfigurert sandmonitroeringssystem levert av ClampOn og arbeidet hadde til hensikt å undersøke utstyrets egnethet til akustisk emisjonsformål. Fra testresultatene kan det konkluderes med at utstyret innehar gode evner til å detektere akustiske emisjoner generert av initiering og vekst av utmattelsessprekker, men at det samtidig mangler verktøy for å filtrere og presentere frekvenser i møte med kontinuerlig støy fra den hydrauliske testriggen.

ABSTRACT

Acoustic emission refers to the dispersal of elastic waves generated by crack initiation and other damaging mechanisms within a material. Recording and analyzing these waves form the foundation of the monitoring technique called Acoustic Emission (AE). The method is widely used in areas such as material research and structural inspection. Furthermore, the method is showing great theoretical and practical promise within the field of fatigue crack monitoring.

In this thesis, the viability of using acoustic emission monitoring for coiled tubing applications is studied through an extensive literature review. The need for fatigue crack monitoring is identified by studying the most influential failure modes as well as the existing inspection technology for coiled tubing. This is followed by identifying potential benefits and challenges of implementing acoustic emission for this purpose, as well as a proposed solution.

Additionally, practical tensile and fatigue cracking tests were conducted on low carbon steel using acoustic emission to monitor damaging processes within the material. The monitoring equipment was provided by ClampOn was a reconfigured sand particle monitoring system and the purpose of the tests was to evaluate the equipment's AE performance. From the test results, it was possible to conclude that the equipment demonstrated an excellent ability to detect acoustic emission generated from the initiation and propagation of fatigue cracks. However, limitations such as lack of frequency filtering and distinction made signal analysis problematic when faced with continuous noise from the hydraulic test rig.

TABLE OF CONTENTS

LIST OF FIGURES

LIST OF TABLES

LIST OF ABBREVIATIONS

AE Acoustic Emission

COTS Commercial off the shelf

CT Coiled tubing

EMI Electro-magnetic interference

HPHT High pressure high temperature

HPU Hydraulic power unit

HSE Health, Safety and Environment

MFL Magnetic Flux Leakage

MPI Magnetic Particle Inspection

NDT Non-destructive testing

RT Radiographic testing

STFT Short time Fourier transform

UT Ultrasonic testing

VFD Variable frequency drive

WT Wavelet transform

1.0 INTRODUCTION

The following chapter describes the demand for condition monitoring of coiled tubing (CT), as well as the potential convenience of utilizing acoustic emission (AE) technology for this purpose. Furthermore, the scope, methodology, limitations and structure of the thesis are described in the following section.

1.1 PROBLEM DESCRIPTION

The global energy demand continues to evolve in line with the world's ever-growing population and with the industrialization of developing countries. Dominant within the global energy matrix is the oil & gas industry, and the industry is forecasted to retain its position for years to come. However, with crude oil prices declining from approximately 100$ a barrel in 2014 to 50$ in 2017, operators search for any means of reducing costs in order to continue profitable production [1]. Paramount in such endeavors, is improving upon existing, or introducing new technology.

Utilizing CT technology in drilling, workover and well-intervention applications is an example of introducing a new approach using existing technology in order to increase efficiency and in turn reduce cost. As a result of its rapid trip speed and ability to operate on pressurized wells, CT is seeing an increasing number of field operations. Furthermore, CT was used extensively and with great success alongside hydraulic fracturing and horizontal drilling to achieve the so called "shale revolution" around the year 2000. However, despite its success the current state of CT technology subjects the tubing string to demanding and inevitably destructive working conditions. Operations include taxing strain cycles that plastically deform the CT string, which can lead to fatigue cracking. These fatigue cracks are one of the leading failure modes for CT operations, negatively affecting the reliability, safety and economy.

The main objective of this thesis is investigating the viability of using AE technology as a condition monitoring method to detect the initiation and propagation of fatigue cracks in CT. Thus, being able to accurately predict and potentially eliminate one the most influential failure modes. Through the process of achieving this objective, related research on existing inspection technology, CT materials, requirements, failure modes and more will be presented.

The process of innovation often includes companies researching outside of their short-term business focus by exploring future applicability of new or existing technology. A good example of this is ClampOn's interest in investigating the possibility of reconfiguring their sand particle monitoring equipment for AE applications. Aiding in this research constitutes the motivation of the secondary objective of this thesis.

The secondary objective is to test, evaluate and provide recommendations for improving, the equipment's AE monitoring performance. This will be accomplished by performing tensile and fatigue tests of low carbon steel while using the equipment to monitor the AE activity related to the development of damaging processes within the material.

1.2 SCOPE

The scope of this thesis is to identify and review existing technology for inspection of CT and to determine the viability of utilizing AE for condition monitoring of CT.

1.3 LIMITATIONS

Every experimental study requires an account of potential weaknesses or limitations that can affect their results. In this study, the following limiting factors were considered while performing tensile and fatigue cracking tests with acoustic emission monitoring:

- Due to the sensitive nature of ClampOn's equipment specifications, and their wish to keep this information confidential, some equipment parameters such as frequency operating range and pre-amplifier gain are unknown.
- The investigated material is limited to the low carbon steel taken from a decommissioned buoy. No other materials will be tested.
- Tools for frequency analysis and filtering were not available, thus limiting the options for removing hydraulic noise.

1.4 STRUCTURE

Described below is the overall structure of this thesis.

Section 1 - Introduction is an introduction to the thesis, providing the problem description, scope, limitations and structure of the performed work.

Section 2 - Methodology describes the methodology used for the literature review and for the laboratory experiments that were conducted in this thesis.

Section 3 – Aspects of coiled tubing provides the necessary background regarding CT in general, materials, manufacturing, current inspection requirements for CT as stated in ISO 13628-7 and the most common failure modes.

Section 4 – Inspection technologies describes the current methods and technology for inspection / condition monitoring of CT. The literature study for this section focuses on the inspection methods application on CT and the literature reviewed includes academic papers, journals, books, master theses and company websites.

Section 5 – Practical results and analysis presents the results acquired from characterizing the noise of the hydraulic test rig as well as from performing tensile and fatigue tests with acoustic monitoring.

Section 6 – Discussion discusses the potential of monitoring CT with AE, the proposed solution, the associated challenges as wells as the results from the laboratory experiments.

Section 7 – Conclusion and recommendations for future work provides a conclusion drawn from the discussion and analysis, as well as recommendations for future work.

2.0 METHODOLOGY

Both a literature review and practical laboratory experiments were conducted in this thesis. The methodology used in completing both segments is described in this chapter.

2.1 LITTERATURE REVIEW

In this thesis, information gathering and research were the primary methods utilized to research the viability of AE as a condition monitoring method for CT applications. The procedure for accomplishing the primary objective of the thesis can be divided into two phases. The first phase of the research includes performing a series of unrestrained searches in the popular search engine *google* as well as discussing the subject with the HVL supervisor and ClampOn representatives. The purpose of this phase is to become familiar with the subject both through discussing the subject with individuals with long time experience in the industry as well as through reading articles and web pages, without substantial concern towards source credibility. Furthermore, this phase grants insight into other people or companies affiliated with the subject.

The second phase of the research procedure consisted of narrowing down search terms in scientific databases and studying the relevant ISO and NORSOK standards used by the industry for CT applications. Through discussion with the HVL supervisor and connections to the industry, it was established that the specific standard *ISO 13628-7 Design and operation of subsea production systems - Part 7: Completion/workover riser systems* is currently used for such applications. Furthermore, searches in the scientific databases of NTNU and HVL provided more detailed insight into different methods of CT inspection. Providing the most relevant and applicable sources of information were the databases *ScienceDirect* and *Engineering village*. Within these databases, tools such as specifying where in the text the search terms should appear, removing duplicates and limiting the publishing date, aid in locating relevant sources. Table 2 is an excerpt of searches made in the scientific database *Engineering Village*. Selection of articles was primarily based on abstract relevancy and in searches with a large number of hits, only the first 50 hits were examined.

TABLE 1 - EXCERPT OF SEARCHES IN *ENGINEERING VILLAGE*

Search words	Database	Section	Date	Number of hits	Selection criteria
Acoustic emission monitoring	Engineering village	Subject/Abstract/Title	21.02.2017	12683	Most relevant abstract: 15
Magnetic flux leakage coiled tubing	Engineering village	Subject/Abstract/Title	21.02.2017	70	Most relevant abstract: 3,5
Ultrasonic inspection of coiled tubing	Engineering village	Subject/Abstract/Title	22.02.2017	43	Most relevant abstract: 4
Radiographic testing of coiled tubing	Engineering village	Subject/Abstract/Title + All fields	22.02.2017	13	No relevant hits
Continuous monitoring of coiled tubing	Engineering village	Subject/Abstract/Title	22.02.2017	85	Most relevant abstract: 1

2.2 LABORATORY EXPERIMENTS

In order to obtain the secondary objective of the thesis a third phase of work was conducted. This phase included practical tensile and fatigue tests with AE monitoring, performed in the HVL laboratory. The phase was completed in cooperation with a BSc group in charge of fabricating test specimens, attaching the transducer and connecting it with the monitoring software provided by ClampOn. The following section describes the method used to evaluate the AE performance of the ClampOn equipment.

2.2.1 EXPERIMENTAL SETUP

This section describes the equipment used in the laboratory experiments.

HYDRAULIC TESTING SYSTEM

For all tensile and fatigue tests, an Instron 8801 servo hydraulic testing system, shown in Figure 1, was used. The rig is capable of applying 100kN of axial force via a hydraulic cylinder and is powered by a hydraulic power unit (HPU) [2]. The wide range different grips and fixtures allowed for proper connection to both the flat tensile test specimens and the K1c fatigue test specimens.

FIGURE 1- INSTRON 8801 SERVOHYDRAULIC TEST RIG USED FOR TENSILE AND FATIGUE TESTS [2]

CRACK OPENING DISPLACEMENT GAUGE

For the fatigue tests, an Instron crack opening displacement gauge was used to measure the crack growth in real time. The gauge provides a precise measure of the increase in relative displacement between two knife-edges, which is converted to actual crack length. The gauge is positioned between two knife-edges that are glued on to the fatigue crack specimen, as shown in Figure 2. For the sake of perspective, it can be noted that the size of the specimen in Figure 2 is approximately 60mm wide, 54mm high and 23mm thick.

FIGURE 2 - INSTRON CRACK OPENING DISPLACEMENT GAUGE MOUNTED ON FATIGUE CRACKING SAMPLE

In accordance to ClampOn's wish to keep detailed information about the acoustic transducer confidential for commercial reasons, only parts of the transducer specification were revealed. The transducer is a piezoelectric resonance transducer originally used for real time sand particle monitoring in pipes [3]. No exact operating bandwidth range has been given, but it is assumed to be similar to others covered in literature which operate in an approximate range of 20 – 1000 kHz.

In order to protect the delicate sensor components, the sensor was glued within a protective housing provided by ClampOn. To ensure satisfactory contact with the test specimen, a custom fastening mechanism was developed, as illustrated in Figure 3, using two large M5 bolts with rubber gaskets to avoid a metal to metal interface.

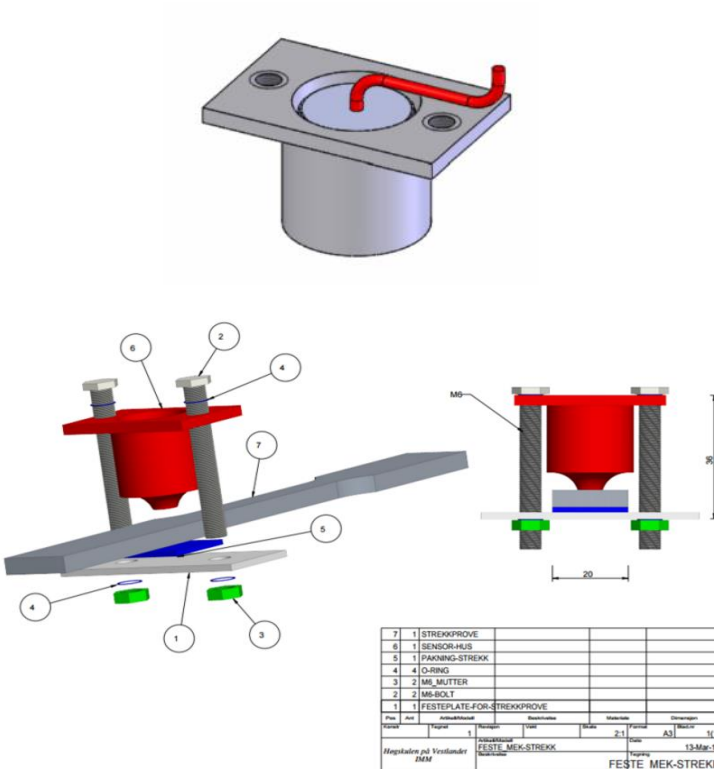

FIGURE 3 - ACOUSTIC SENSOR AND FASTENING MECHANISM

The cable from the transducer was connected to a pre-amplifier, also provided from ClampOn. Again, for commercial reasons, ClampOn could not share details about the specification of this pre-amplifier. Consequently, the amplification and band-pass filter frequencies of the pre-amplifier are unknown. The pre-amplifier is powered by a power supply which is connected to a 230V wall outlet through a AC-C13-EU cable. Figure 4 shows the SandQ transducer, the preamplifier and the power supply.

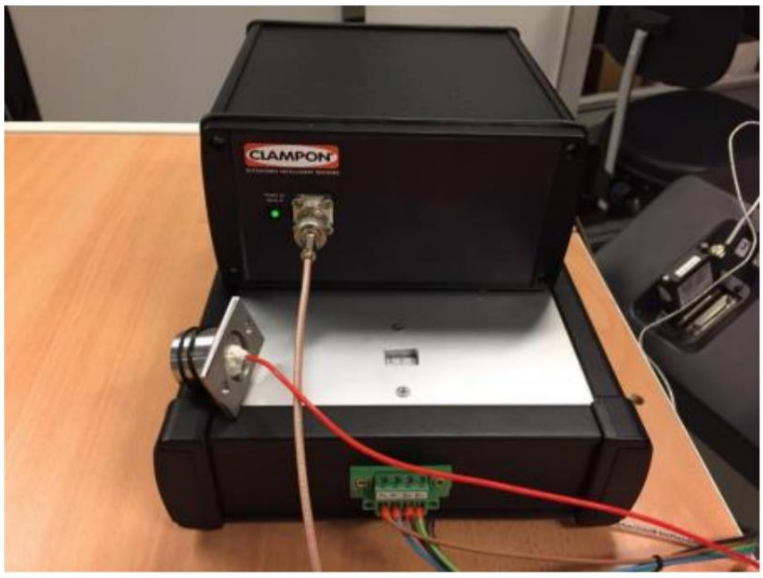

FIGURE 4 - POWER SUPPLY, ACOUSTIC TRANSDUCER AND PRE-AMPLIFIER

SOFTWARE

The software used for acquiring AE data from the transducer is a beta-version created by ClampOn specifically for the cooperation project between HVL and ClampOn, this semester. The software combines a user-friendly interface with an ordered overview of measured parameters. It allows for visualization of amplitude, rise time, absolute energy and cumulative energy with regard to time. Furthermore, individual hits can be can be selected and analyzed. However, as will be discussed later in the thesis, the software does have some limitations concerning frequency visualization and filtering.

SPECIMENS

Exact material properties such as E-modulus, Poisson ratio and tensile strength of this steel were unknown and it was decided to perform tensile tests to determine these values. Three separate tests were conducted, of which the average values are presented in Table 2. These values were later used in the hydraulic test rig software to achieve the desired rate of deformation.

TABLE 2 - AVERAGE OF MEASURED MATERIAL PROPERTIES

Average E-module [GPa]	Average Yield strength [MPa]	Average Tensile strength [MPa]
208	348	430

The tests were done using three circular tensile test specimens machined, shown in Figure 5, from the same steel block as the rest of the test specimens. The specimens were machined in compliance with the NS-EN 10002-1 standard. In order to obtain information regarding processing and rolling of the steel, one of the specimens was machined at a 90-degree angle and two specimens at 45-degree angle relative to the steel block.

FIGURE 5 - CIRCULAR TENSILE TEST SPECIMENS

In addition to the three circular tensile test specimens, three flat shouldered tensile test specimens, in compliance with ASTM E8/E8M-13, were machined. These were to be used for tensile tests and load hold tests with AE monitoring. The flat shoulder design was selected to allow the coupling of the AE transducer on the specimens during the tensile and load hold tests.

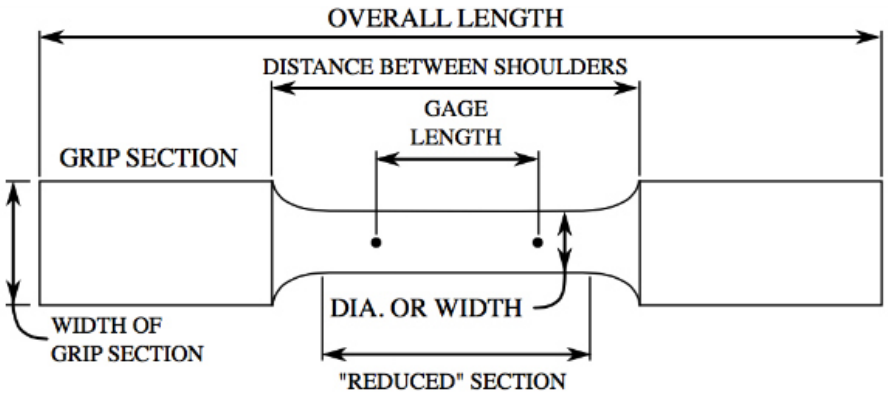

FIGURE 6 - FLAT SHOULDERED TEST SPECIMEN

In order to obtain consistent and reproducible fatigue test results, it was decided to comply with the ASTM E339 standard for machining fatigue crack test specimens. Within the standard several designs for test specimens are described. Due to the difficulty of machining the triangular cracked specimen with the tools available at HVL, it was decided that the circular cracked specimen was to be used, illustrated in Figure 7. Furthermore, a small crack starter notch was sawed into the centerline of the machined circle on some of the specimens. The specimens were machined from blocks of low carbon steel, taken from a decommissioned buoy.

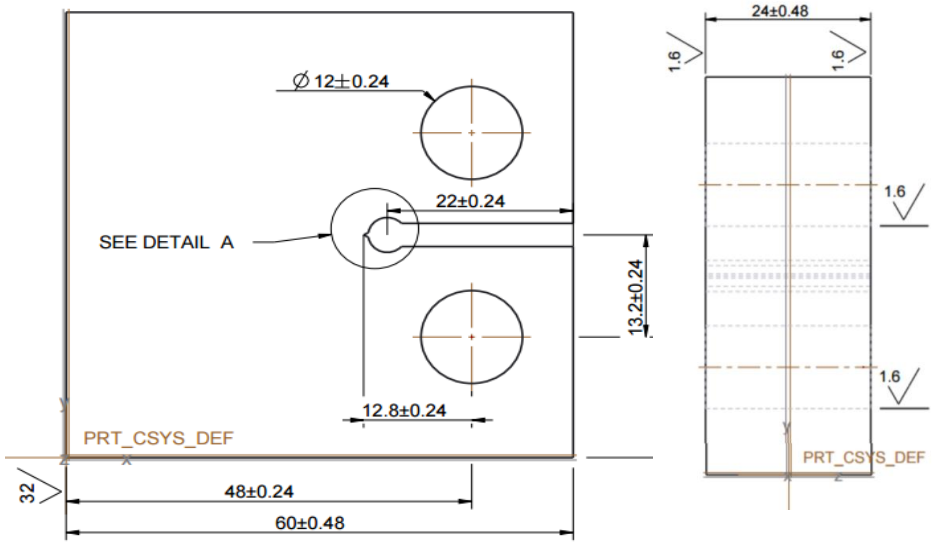

FIGURE 7- TRIANGULAR AND CIRCULAR CRACK FATIGUE SPECIMENS

2.2.1 PROCEDURE

After connection between the sensor and the AE software had been achieved, the sensor was attached to the test specimen using the custom fastening mechanism in combination with electrical tape. Furthermore, a thixotropic paste was used as a couplant to ensure proper wave transmission from the specimen to the sensor.

To verify adequate connection between sensor and the test specimen, as well as proper sensor calibration, a standard pencil break test was performed. A recorded peak amplitude value of 65 dB or higher was considered an acceptable pencil break result, if the value would have been lower the sensor would be re-attached. Figure 8 is a snapshot showing the waveform of a pencil break test signal, with amplitude in µV plotted versus time in µS. Also shown in the figure is the value of peak amplitude, which was 70,8 dB for this signal.

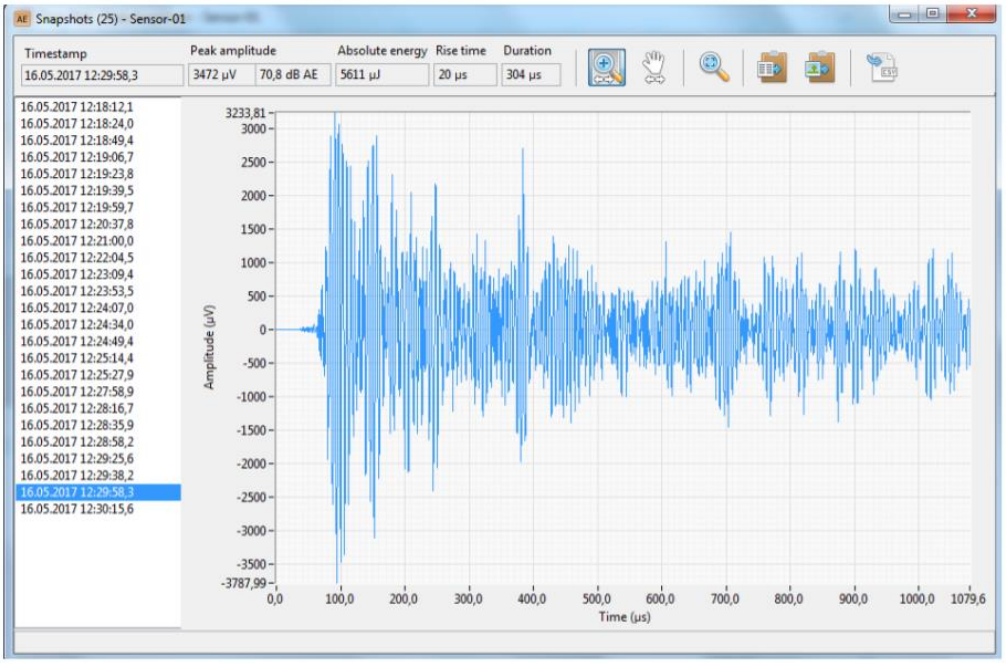

FIGURE 8- SIGNAL WAVEFORM OF PERFORMED PENCIL BREAK TEST

For the tensile test specimens, the AE sensor was attached with an offset to the elastic area, as shown in Figure 9(left), in order to not interfere with deforming area. For the fatigue test specimens, the sensor was attached on the backside directly across for the machined crack as shown in Figure 9(right). After attaching the sensor, the specimens were placed in the test rig and carefully aligned to the correct position. Finally, the test program was initiated simultaneously with the AE monitoring software in order to compare occurring events with regard to time. Three different types of tests are described in the next section.

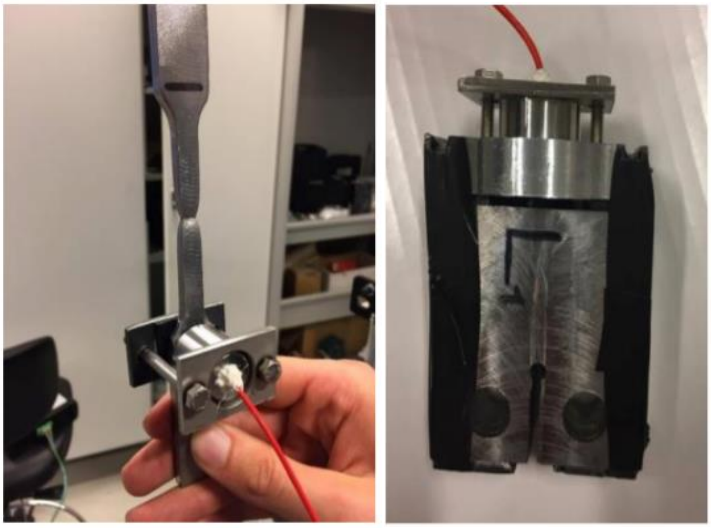

FIGURE 9 - AE SENSOR PLACEMENT ON TENSILE TEST SPECIMEN (LEFT) AND AE SENSOR ON FATIGUE TEST SPECIMEN (RIGHT)

TENSILE TEST

The first tensile test was set to subject the specimen to a linearly increasing deformation. The deformation speed was set to 1,2mm/min, based on the material properties from Table 2.This deformation speed is slightly slower than for regular tensile tests in the HVL laboratory, which are performed at 1,5mm/min. The speed was selected in order to increase the observation time of potential activity within the elastic area. The resulting time to failure using this deformation speed was 630 seconds.

STEPWISE TENSILE TEST

The second tensile test was completed using a stepwise load program with offloading in between the loads. The force steps were 25% (4500N), 50% (9000N) and 80 % (14400N) of the yield strength acquired from the preliminary tensile tests without AE monitoring. The duration for this test amounted to 90seconds.The motivation for performing this stepwise test was to recreate and study the Kaiser-effect (discussed in section 4.5.2)

FATIGUE TEST

For the fatigue test, a preliminary test was conducted to establish specific test parameters, such as force, frequency and final crack length, that would provide an adequate result within an acceptable time frame. The concerns were that if the applied force was too low, the test would go on for too long. This would be problematic with regard to available time in the HVL laboratory as well so for the file size from the AE software. Furthermore, a suitable final crack length had to be established in order to avoid the backside of the specimen from bending thus losing connection to the sensor or even possibly damaging the attached sensor.

From the results of the preliminary tests without AE, it was determined to run the first of the two tests with AE monitoring at 50kN applied force, a frequency of 5Hz and with a final crack length of 30mm or until the gauge's maximum displacement had been reached. With these parameters, the test time amounted to approximately 45 minutes. In order to investigate a possible source of AE activity prior to crack development, it was decided to run the second fatigue test using a specimen without an induced crack.

The second test was conducted with an applied force of 35kN and with the same settings for frequency and crack length. With these settings, the test time for the second test approximately 2hours 45 minutes. The purpose of conducting fatigue tests at different loads, was to study different AE activity between a low cycle fatigue cracking test and a high cycle fatigue cracking test.

3.0 ASPECTS OF COILED TUBING

A fundamental understanding of CT technology is required in order to investigate the viability of using AE to monitor damaging processes associated with its use. As such, this section provides necessary background information concerning CT in general as well as materials, fatigue life, inspection and failure modes. The Non-destructive testing (NDT) methods presented in this section will be further described in chapter 4.

3.1 COILED TUBING

As previously mentioned, CT is seeing an increase in applications as operators emphasize the need for rapid and cost-effective solutions for drilling and workover applications [4]. Furthermore, key benefits of utilizing CT such as reduced personnel requirements and reduced trip time / rig-up, continue to spur further application and development of the technology.

CT can essentially be described as continuous lengths of milled pipe, featuring flexible properties allowing it to be spooled on a large diameter reel [4]. During operations, the CT string is unwound from the reel and inserted into the wellbore. Prior to wellbore insertion, the CT string is straightened through a gooseneck and upon retrieving the string; it is recoiled onto the reel. Typical dimensions for CT strings include outer diameters in the range of one to five inches, wall thicknesses in the range of 0.08 to 0.3 inches and lengths upwards of 30 000 feet [4].

Originally, CT served as a niche solution to specialized service and workover problems. However, over time manufacturing companies have continued to evolve the technology by increasing manufacturing quality, improving service reliability, decreasing cost and gradually increasing CT string diameters [5]. Consequently, CT has seen an increase in viable applications such as drilling, high angle borehole logging, workover, wellbore cleanouts, acid or fracture stimulation, downhole monitoring etc. [5]. CT drilling is one of the branches showing significant promise for the future and successful applications in the field.

An example is Iceland Offshores open water CT system, which in 2014 successfully drilled core samples through a monohulled vessel north off the shore from Stavanger [6]. In 2015, the same company completed a shallow gas pilot hole drilling operation for Centrica Energy, drilling 360 meters below the mudline north of Ekofisk.

Key components of a CT unit consist of the following:

- Reel – used for storage and transportation of CT string
- Gooseneck – guides and aligns the CT string vertically with the injector head
- Injector head – provides the necessary drive to run and retrieve the CT string
- Power supply – provides the necessary power to operate all CT components

FIGURE 10 - OFFSHORE COILED TUBING CONFIGURATION [7]

3.2 COILED TUBING MATERIALS

The material used for CT strings can vary depending on operating conditions and with special cases such as sour service or HPHT wells [8]. However, numerous requirements for CT steel grades are specified in API SPEC 5ST. The standard classifies the steel grades for all carbon and low alloy steels, by their minimum yield strength in psi; CT 70 – 70 000 psi, CT 80 – 80 000 psi and so on up to CT 110 – 110 000 psi. Within these categories there are defined requirements for chemical composition with regard to mass percent of carbon, manganese, phosphorus, sulfur and silicon. Furthermore, the CT steel grades are required to conform with the standards values for hardness and grainsize as well. Figure 11 shows the proposed material qualities according to API RP5C7 [9]

Not specified within the standard are alternative materials such as composites or aluminum. This is largely due to the fact that they are still in a development phase and thorough documentation and testing remains to be completed before the technology breaches the first user barrier. However, composites do show significant promise with qualities such as corrosion resistance, chemical inertness and embedded fiber optics, thus making reasonable to believe it will see more use in the future.

TABLE 3.18—PROPOSED TENSILE AND HARDNESS REQUIREMENTS FOR COILED TUBING

	Yield Strength* (psi)		Ultimate Tensile (psi)		Maximum Hardness Body Hardness-
Grade	Minimum	Maximum	Minimum	Maximum	Rockwell C
CT60	60,000	75,000	70,000	90,000	22
CT70	70,000	85,000	80,000	100,000	22
CT80	80,000	95,000	90,000	105,000	22
CT90	90,000	105,000	98,000	115,000	23
CT100	100,000	115,000	108,000	125,000	26

*Spooling and unspooling can result in a reduction of the yield strength of approximately 5 to 10%.

FIGURE 11 - TENSILE AND HARDNESS REQUIREMENTS FOR COILED TUBING [9]

3.3 COILED TUBING MANUFACTURING PROCESS

The manufacturing process of CT initiates by acquiring wide steel sheets (40-48 inches) and wrapping them on a large coil, often referred to as the "master coil" [10]. These sheets are then put in a strip and are slit to a width corresponding to the desired circumference of the final tubing. From there the skelp ends are welded together forming a continuous steel length and inspected for defects. A series of rollers gradually work the steel sheets mechanically into a tubular shape and leave the tube edges close together. High frequency induction welding (HFI) join the two edges together by generating heat from resisting the flow of electrical current and pressing them together using forming rollers [10].

FIGURE 12 - SLITTING STEEL SHEETS FOR CT [10]

The exterior weld flash (steel bead) is then removed and the seam is annealed. The tube is air cooled followed by a liquid cooling bath prior to NDT of the tube body. The eddy currents method is commonly used for this purpose [10]. The final stages of CT manufacturing include passing the tube through a sizing mill that ensures the correct tolerances and outer diameter to match costumer requirements. During this period, the tube is heated in order to relieve the material of stresses, thus

increasing the ductility of the tube. Letting the tube cool in air followed by a liquid bath allows the development of pearlite and ferrite, resulting in a high-strength CT string matching the physical property requirements of the API standard [10].

While there are alternative methods to manufacture CT strings, such as butt-welding tubular sections together, the skelp welding method is the most common [10].

3.4 COILED TUBING FAILURE MODES

Conventional CT drilling or well-intervention operations subject the CT string to cyclic bending and deformation within its range for plastic yield [11]. These bending events occur a total of six times during one trip occurring at three different locations in the CT configuration. Figure 13 illustrates the configuration and locations of the three bending points. Furthermore, some drilling or intervention operations perform “drag checks”. These involve periodically stopping the tube deployment and reversing the motion so that drag and weight may be measured [11]. Consequently, intermediate sections are subjected to a larger number of trips than the string as a whole, resulting in a greater accumulation of fatigue damage. Such bending behavior can result in ultra-low cycle fatigue cracking. Formation of micro cracks in the pipe wall is a consequence of the ultra-low cycle fatigue. Continued bend cycling causes these cracks to propagate until full penetration is established and pressure integrity is lost rendering the string unfit for further operations. Furthermore, uneven diametric growth causing ovality of the CT string can drastically reduce its collapse pressure rating [11]. This phenomenon occurs as a result of cyclic bending in combination with internal pressure loading and is called ballooning.

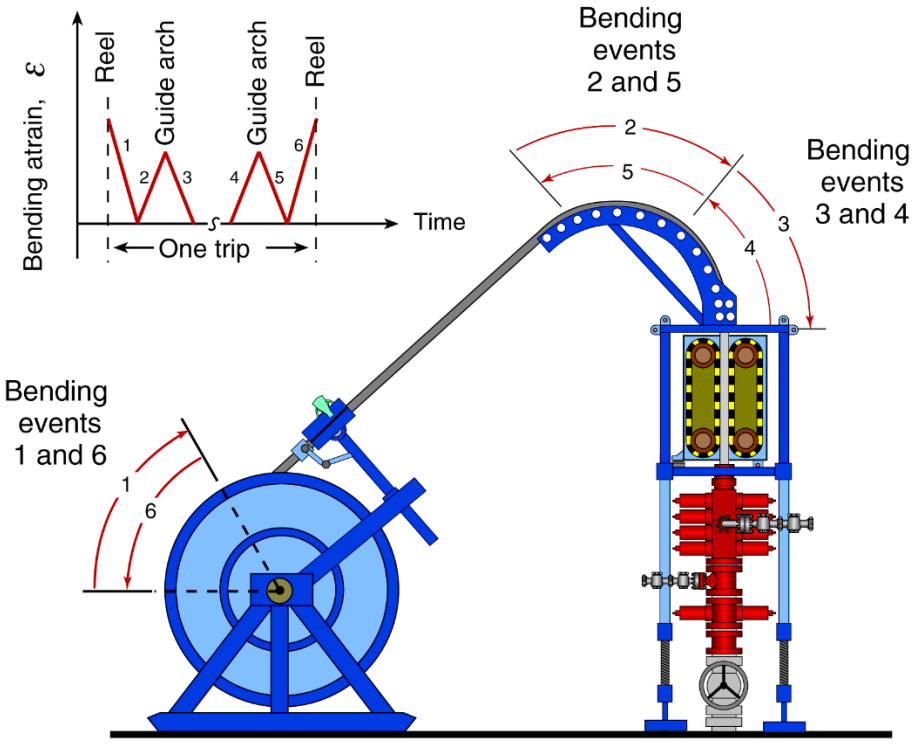

FIGURE 13 - COILED TUBING BENDING EVENTS [11]

In addition to the cyclic bending, the CT string is exposed to several other factors contributing to a reduction of the strings service life and potentially leading to failure. Such factors include internal pressure loading and axial tension caused by the weight of the string [11]. Corrosion, both pitting and uniform, from exposing the string to seawater and mechanical damage such as scratches, dents and gouges. Individually and synergistically, the above-mentioned factors can lead to failure of the CT string.

A study published by the society of petroleum engineers, systematically analyzing more than 360 CT field failures from 1995 to 2001, provides valuable data exposing the most frequent failure modes [12]. The failure modes are divided into 9 categories as listed below, and their frequency of occurrence is presented in Figure 14.

- M1 - Tensile overload
- M2 - Buckling
- M3 - Rupture: CT failed because of excessive internal pressure
- M4 - Collapse: CT failed because of excessive external pressure
- M5 - Fatigue: CT failed because of fatigue crack initiation and propagation
- M6 - Material loss: CT cannot be used because of wall thickness loss
- M7- Distortion: CT cannot be used because of its shape or size change, such as ballooning, diameter reduction, etc.
- M8 - Mechanical damage: CT cannot be used because of significant mechanical damage (dents, gouges, etc.)
- M9 - Other: Failures other than those listed previously

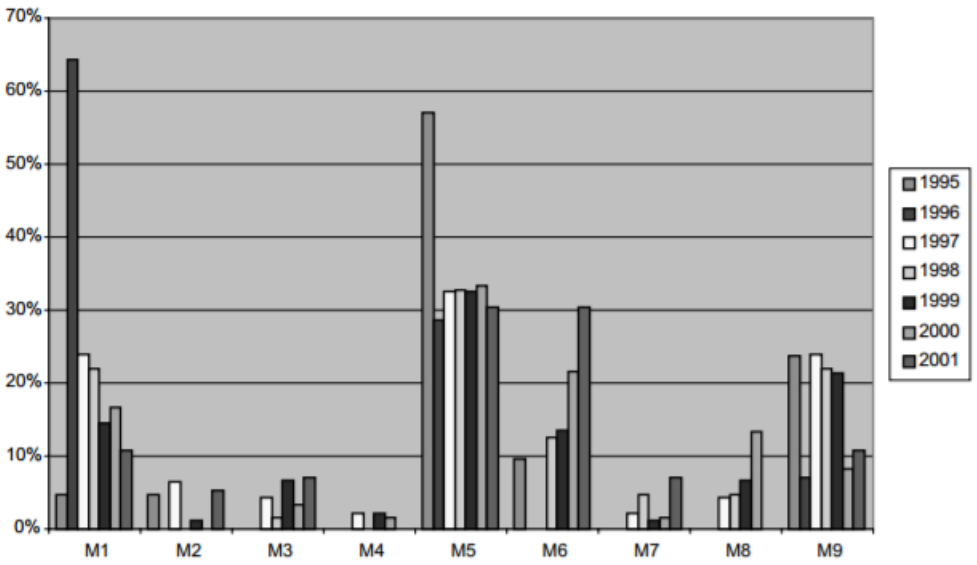

FIGURE 14 - FAILURE MECHANISM TRENDS FROM 1995 TO 2001 [12]

From Figure 14, it becomes evident that the most influential failure modes with regard to occurrence are M1: Tensile overload, M5: Fatigue cracking and M6: Material loss. These failure modes show the highest frequency of occurrence by a substantial margin. The information gained from such a study, can be further used to establish which parameters should be monitored to determine CT string condition and to avoid the occurrence of the common failure modes. For this thesis, it serves as a strong argument for why fatigue crack monitoring is of importance.

3.5 COILED TUBING FATIGUE LIFE AND INSPECTION REQUIREMENTS

ISO 13628-7 2006 defines requirements for completion/workover riser systems and is also applied to CT applications. The standard does not propose fatigue monitoring, rather it specifies directions for fatigue life analysis and selection of NDT intervals and methods. Cumulative damage and/or crack growth analysis may be used for fatigue life analysis, thus forming the basis for the fatigue crack inspection program of the CT [13]. Furthermore, a design fatigue factor shall always be implemented for the calculated fatigue life, as shown in the equation below [13].

$$\frac{L_F}{D_F} \geq L_s$$

For inspection, the standard specifies NDT techniques depending on material and imperfection type. Magnetic particle inspection (MPI) with the wet fluorescent method is preferred for ferromagnetic materials with surface imperfections. For non-magnetic materials however, eddy currents or dye penetrant is preferred [13]. Internal imperfections are to be inspected using either radiographic and/or ultrasonic testing (UT). These two methods may supplement each other in order to enhance characterization, sizing or detection probability of the internal imperfections. Preferred for detection of internal volume imperfections is the radiographic testing (RT) method, while UT is generally preferred for internal planar defects [13].

UT is generally not applicable for thicknesses less than 10mm, thus it may be necessary to replace it with RT [13]. For thicknesses exceeding 25mm however, it may be necessary to supplement RT with UT. Lastly, UT may be required for accurate height and length assessment of fractures.

The standard also states that alternative detection methods may be utilized, provided that the method has demonstrated its capabilities of imperfection detection at similar levels of the previous proposed methods.

With regard to monitoring, the standard does not deem it mandatory for the C/WO riser itself but rather the sea state and operating conditions.

4.0 INSPECTION TECHNOLOGIES

The purpose of this chapter is to familiarize the reader with the currently available inspection / monitoring methods for CT as well as their limitations, thus revealing the potential for AE monitoring. This is done by presenting their working principle as well as their limitations. Then, AE basics, sources, equipment and limitations are described.

The following methods will be covered chronologically:

- Magnetic flux leakage
- Magnetic particle inspection
- Radiographic testing
- Ultrasonic testing
- Acoustic emission

4.1 CURRENT INSPECTION TECHNOLOGIES

4.1.1 MAGNETIC FLUX LEAKAGE

A proven and widely popular NDT technique for CT strings is the Magnetic Flux Leakage (MFL) method. The method can operate without requiring surface preparation or coupling between sensor and monitoring surface [14]. Consequently, the method has no issue monitoring a muddy or wet surface, thus making it suitable for use in an offshore environment. Furthermore, it is able to detect both interior and exterior surface defects. The working principle in MFL inspection relies on magnetizing the ferromagnetic pipe material to approximately saturation values. This is achieved by applying a magnetic field using a permanent magnet as an excitation source. Magnetic flux lines will travel through the ferromagnetic pipe material, flowing from the south pole of the magnet to the north pole [14].

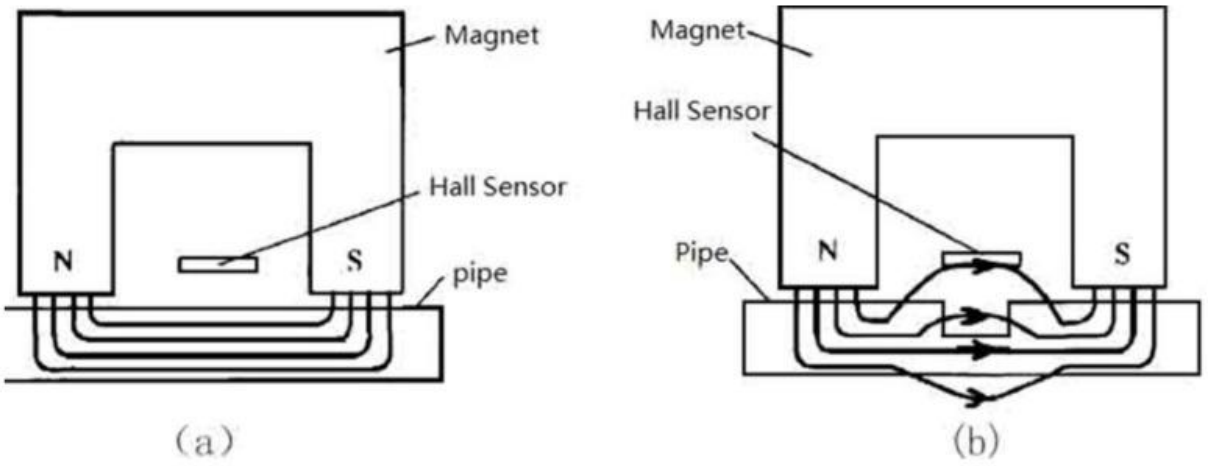

FIGURE 15 - MAGNETIC FLUX LEAKAGE PRINCIPLES [14]

Should the pipe wall be damaged by scratches, gouges, dents or similar, the reduced magnetic permeability of the defect area will cause an increase in magnetic resistance. The result is a distortion of the magnetic field in the defect region. The distortion bends the magnetic flux lines causing some of them to leak from the material entirely. These evading flux lines create a leakage field that can be detected using a magnetic sensitive sensor, in most cases a Hall sensor [14]. Figure 15 illustrates the basic MFL principles through a simplified configuration where figure (a) shows a pipe without defects and figure (b) shows a pipe with a defect. As can be seen, the magnetic flux lines in Figure 15 (b) are clearly distorted and leak out of the inspected material.

After a leakage field has been created surrounding a defect, the field's vector distribution can be mapped as shown in Figure 16. Each component is presented individually in a diagram where the defect width is represented by the horizontal axis and the magnetic induction intensity is represented by the vertical axis. This allows for a simple representation of the pipe defect.

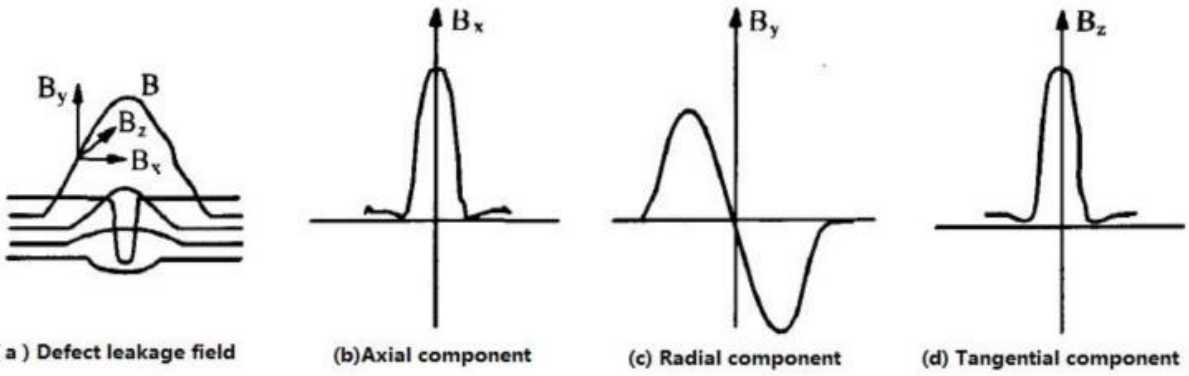

FIGURE 16 - COMPONENTS OF DEFECT LEAKAGE FIELD [14]

However, more advanced representations are available in 3D signature plots of the leakage field surrounding the defect. Such representations may simplify the qualitative analysis the operator has to perform in order to characterize defects. Figure 17 shows a 3D representation of a CT string bias weld anomaly with respect to MFL amplitude, circumference and depth.

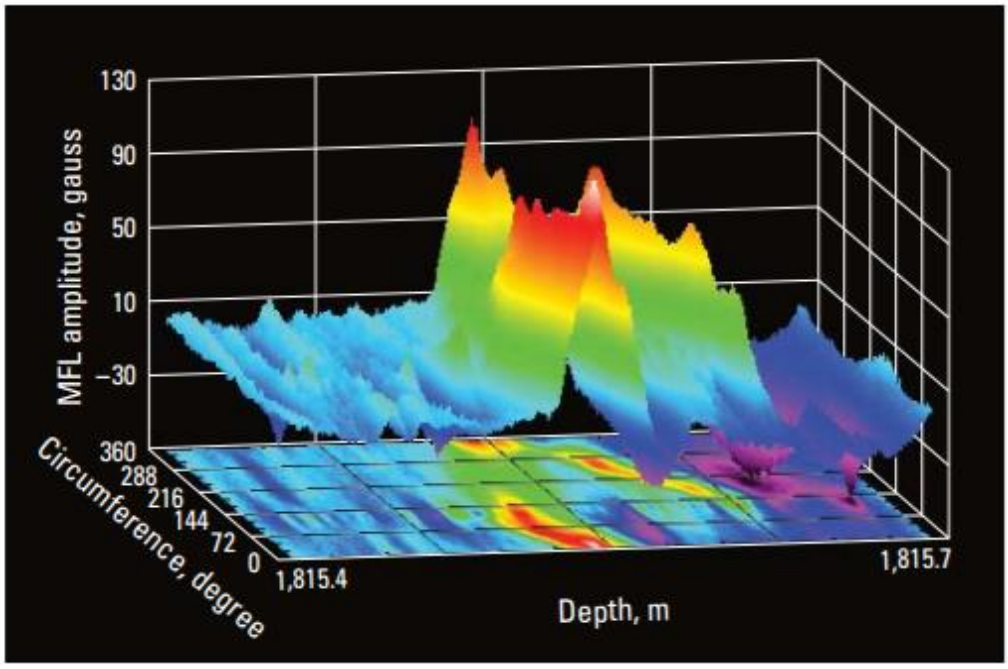

FIGURE 17 - 3D MFL PLOT FOR BIAS WELD ANOMALY [14]

LIMITATIONS

As mentioned previously in this section, the MFL inspection technique offers some desirable attributes. These attributes include not requiring coupling with the inspected surface or pre-processing of the acquired signal. Furthermore, the method features a high level of versatility in defect detection ranging from surface defects to shrinkage cavities [14].

However, the method is also effected by several limitations. The most influential limitation is the level of qualitative analysis that is required in order to identify and characterize defects. Some defects can be complex to characterize and may require both time and skill from the operating personnel. Furthermore, due to the used of magnetic field lines, the inspected material must be ferromagnetic thus excluding some of the more innovative pipe materials such as aluminum or composites. Lastly, narrow defects such as internal cracks, especially axial cracks, are difficult to detect using MFL [14]. This becomes a severe limitation in CT applications, as it from section 3.4 was demonstrated that fatigue cracking was one of the most frequent failure modes.

4.1.2 MAGNETIC PARTICLE INSPECTION

MPI is the preferred method for detecting surface defects in ferromagnetic materials according to ISO 13628-7. The method is largely a combination of the previously presented MFL method and visual inspection [15]. The working principle is similar to MFL, as it involves magnetizing the object to be inspected to saturation levels, thus creating magnetic flux lines that travel through the ferromagnetic material. The presence of surface defects such as cracks or gouges will cause a spread in the magnetic field and create a flux leakage field, as shown in Figure 18. However, instead of detecting these evading flux lines through the use of magnetic sensors, magnetic particles in dry powdered form or suspended in a liquid are released on the magnetized surface [15]. These magnetic particles are commonly made from iron, and are mixed with fluorescent/colored particles. These particles will cluster around the flux leakage field, thus making the defect visually easier to locate for the inspector.

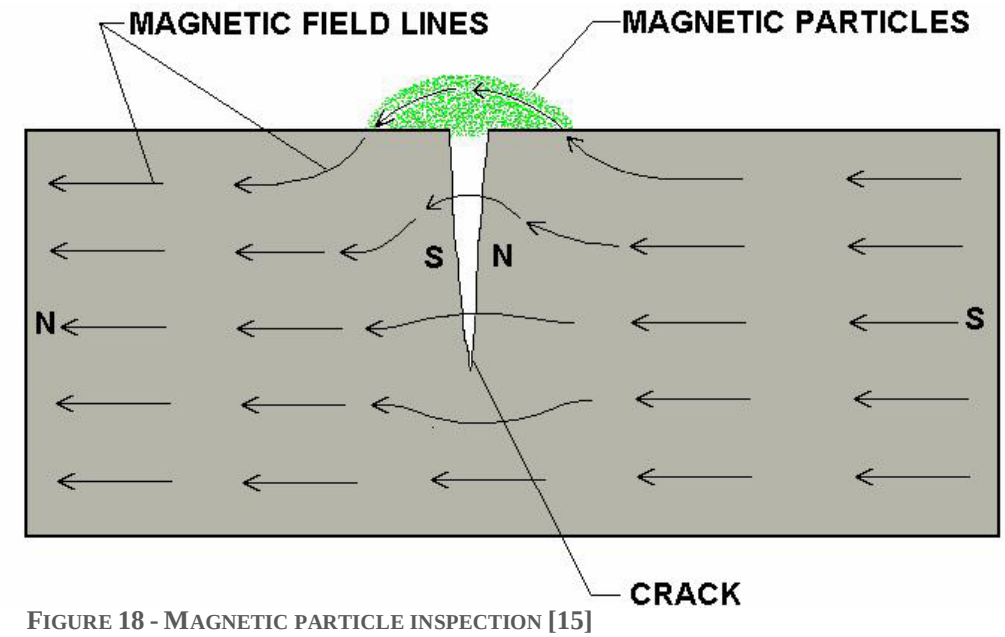

FIGURE 18 - MAGNETIC PARTICLE INSPECTION [15]

The magnetization of the inspected part may be produced by various methods [15]. Two of the most commonly used methods include either utilizing a permanent or electromagnet to create magnetic flow or by passing current through the inspected part.

After either of these methods have been applied, it is commonly necessary to demagnetize the inspected part. This is to avoid unwanted effects such as cuttings or abrasive particles clinging to areas of the component or it interfering with electronic equipment as a result of the remnant magnetic field. Similar to magnetization, demagnetization can be achieved in several different ways. However, the two most commonly used methods include heating the material to above its curie temperature or subjecting the material to a reversed and slightly decreasing magnetic field.

LIMITATIONS

As mentioned previously with MFL, MPI is also limited to use on ferromagnetic materials, thus excluding some of the more innovative materials like aluminum or composites. Furthermore, the mobility of the magnetic particles used in the inspection can be compromised by rough, dirty or painted surfaces. This reduction in mobility can ultimately reduce the flaw detection sensitivity [15]. After the testing is completed, cleaning and demagnetization is usually required which can be time consuming and inconvenient for large structures.

4.1.3 RADIOGRAPHIC TESTING

RT is the second example of a well-established NDT method for a wide range of applications, including welds, pipes and tubulars. Considered second only to visual inspection with regard to usage, RT has been and is still being used by companies worldwide [16]. The working principle of the method consists of passing radiation through the solid object to be inspected. As the radiation penetrates through the material, parts of the energy are attenuated through interactive processes including absorption and scattering. The amount of attenuated energy is dependent on both thickness and density of the inspected material. Either a digital detector or a conventional photographic film is used to capture the energy that passes through the material. For applications using photographic film, the radiation hits the photographic film on which a black and white image of materials internal structure is deposited. White areas on this photographic film appear as a result of energy that has not been absorbed by the material. Dark areas however, are a result of less energy exposing the photographic film. If a digital detector is used, these color effects are reversed. Consequently, light areas appear as a result of absorbed energy and dark areas as a result of unabsorbed energy. These images are often referred to as "positive" images. In order to avoid misinterpretation of the acquired RT results, the operator must be aware of which of the two techniques is being used.

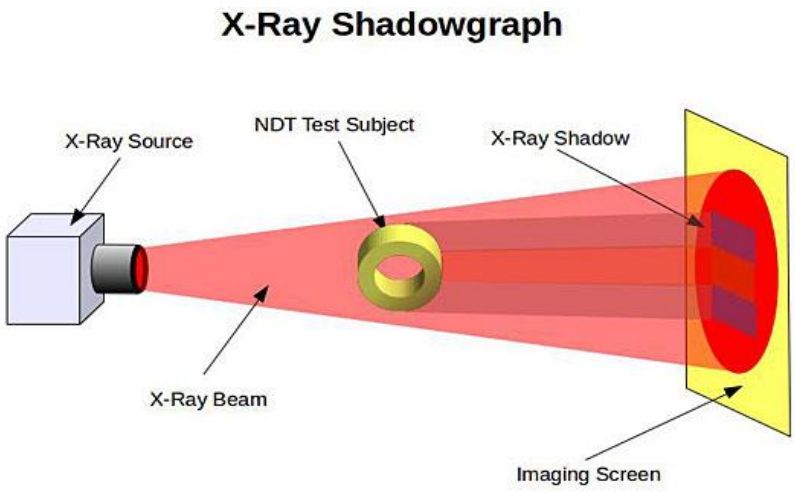

FIGURE 19 - ILLUSTRATION OF RT PRINCIPLE [17]

Two radioactive sources form the basis of industrial RT: X-rays and gamma rays. X-rays are electromagnetic radiation waves with up to 100,000 times as much energy as visible light. The combination of high energy, low wavelength and high frequencies, allows the x-rays to pass through solid matter [16]. Gamma rays are emitted during the breakdown and decay of unstable nuclei. Similar to x-rays, they are able to penetrate and pass through solid matter. It should be noted that several factors dictate the amount of radiation, be it x-ray or gamma, which can pass through a given material. Such factors include material composition, thickness, density and the wavelength of the electromagnetic radiation [16].

RT offers numerous advantages that make the method viable in a wide variety of applications. Such advantages include not being limited by the material to be inspected, as the method is applicable for most material types. Furthermore, the full thickness of the inspected object is tested at once and with high sensitivity to changes in density or thickness [16]. Lastly, the test provides a permanent documentation record as the results are in the form of photographs.

LIMITATIONS

A number of limitations with regard to application, detection and HSE also affects RT. Primarily, extensive safety precautions are required for safe operation due to the high intensity radiation present during inspection. Lack of caution while operating RT equipment can lead to severe consequences for both the operator and workers within the vicinity [16]. Furthermore, the method requires extensive technician training prior to inspection in order to efficiently and reliably analyze the acquired results. As for detection, RT is proficient at detecting volumetric defects but not suitable for detecting planar defects.

4.1.4 ULTRASONIC INSPECTION

Widely popular and established for industrial applications is the UT inspection method. The method is mainly used for larger pipe inspections, but has been modified and adapted for CT applications.

UT inspection utilizes the propagation of ultrasonic sound waves through the target material, to determine diametric variations, defects, material characterization, anomalies and more. Typical configurations of the UT inspection method, includes using one or more UT probes that are coupled acoustically with the pipe or tubular. Such probes contain a UT transducer, which generates high-energy UT waves, and a receiver. The transducer and receiver can be housed in the same probe, or alternatively in two separate probes at different locations [18].

Ultrasonic transducers are almost exclusively made from piezoelectric materials, originally in the form of quartz (SiO_2). The quartz crystal consists of Si-atoms surrounded by four O atoms in a tetrahedron shape. Today, piezoelectric ceramics like lead zirconate titanate, also called PZT, are the most common transducer materials. These materials are polarized and an electrical charge will be generated if it is compressed [19]. This is called the piezoelectric effect. Placing the piezoelectric material between two metal plates and applying AC voltage between the two plates causes the material to oscillate matching the frequency of the voltage and emitting longitudinal waves into the underlying material. This is called the inverse piezoelectric effect and is the working principle of most UT transducers.

The resonant frequency of a piezoelectric disc is inversely proportional with its thickness. If the thickness is **d** the resonant frequency becomes $\mathbf{f_r = c/2d}$. When the material is excited either electrically or acoustically at this specific frequency, the vibrations become stronger than with other frequencies [19].

Within solid matter there are several types of acoustic waves that can propagate. Longitudinal waves, also known as pressure waves, consist of periodic compression within the material propagating with a certain velocity. Particles within these waves move the same direction as the propagating wave increasing and decreasing pressure as they go [19]. In transverse waves, the particles oscillate perpendicular to the wave motion. Surface waves are mechanical waves that propagate across an interface between two different media. Longitudinal and transverse waves form the basis of UT inspection, while surface waves play a crucial role in AE monitoring [19].

The most common method for UT inspection is called the pulse-echo method. In this method, a transducer generates an acoustic pulse with a frequency of approximately 1MHz and a travel velocity in steel of approximately 6000m/s [19]. Between 500 to 2000 pulses can be emitted in one second. As the emitted pulse from the transmitter propagates through material and encounters a defect, some of the energy is reflected by the defect area. The reflected signal is illustrated using an oscilloscope with regard to time and amplitude. This allows for analysis of the defect characteristics including size, location and orientation.

Figure 20 shows an oscilloscope reading of an UT-signal propagating and reflecting through a stainless-steel block. The x-axis of the oscilloscope reading shows time while the y-axis shows signal amplitude. The reading illustrates one distinct signal originating from the reflection of the end of the steel block. This indicates that there are no detectable defects at this location.

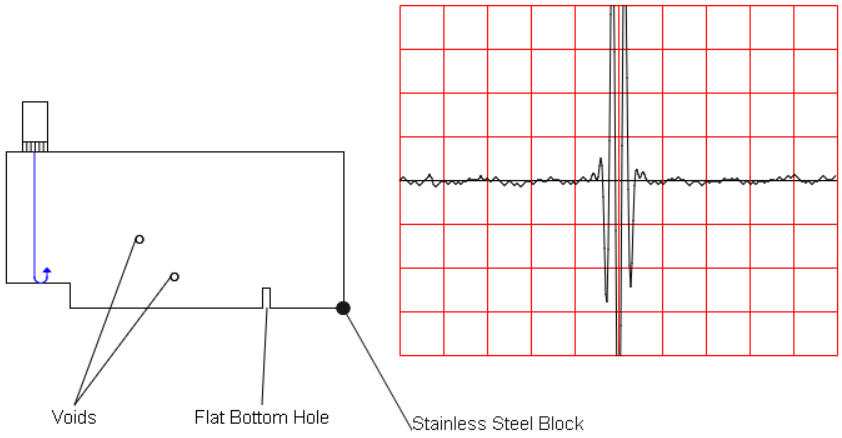

FIGURE 20 - OSCILLOSCOPE READING OF REFLECTED SIGNALS [18]

Figure 21 shows the oscilloscope reading of the same steel block, but with the probe at a different location. The figure shows the acquired signal is further to the right, which means that more time has passed between sending the signal and receiving its reflection. This is to be expected as the UT waves travel a larger distance than in Figure 20. However, only one distinct reflection is received, indicating that there are no detectable defects in this location either.

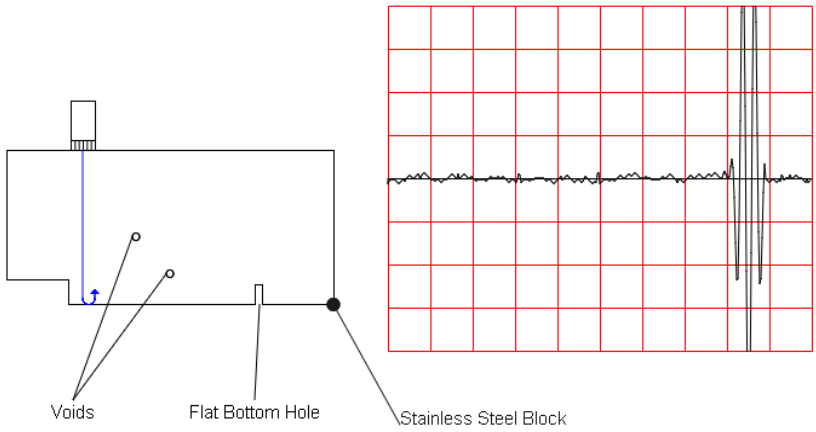

FIGURE 21 - OSCILLOSCOPE READING OF REFLECTED SIGNALS [18]

Finally, Figure 22 shows the oscilloscope reading of the same stainless-steel block at a third location. In this scenario however, two distinct reflections can be observed at different time intervals. This is caused by the UT signal partially reflecting from the void inside the steel block as well as from the end of the block.

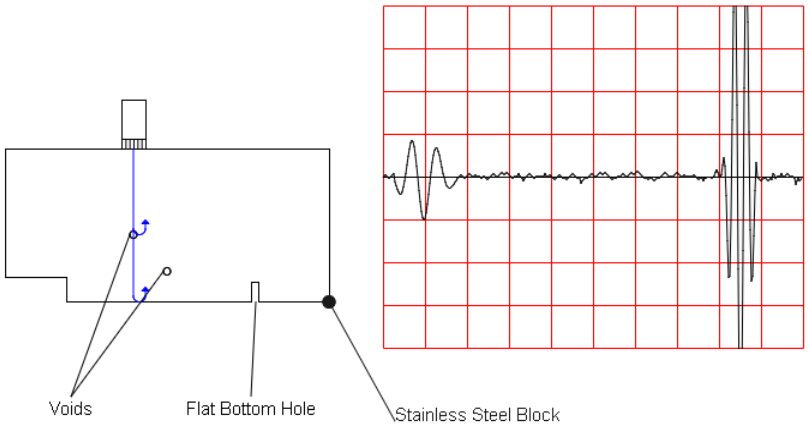

FIGURE 22 - OSCILLOSCOPE READING OF REFLECTED SIGNALS [18]

Utilizing UT offers several advantages that make the method highly valued within the NDT category. Such advantages include the high level of portability for the required equipment, high sensitivity and considerable signal penetration depth. This allows the method to detect very small internal discontinuities deep within the inspected material. Furthermore, the method is applicable on most materials, including biological materials, metals and ceramics [19]. Minimal preparation is required and poses no health or environmental risk during any course of the operation.

LIMITATIONS

As with any NDT method, there are limitations to the UT method that are important recognize. Firstly, UT results are greatly dependent on operator skill and qualifications. This implies that certain defects can go undetected as a result of human error or inexperience. Consequently, UT requires training that is more extensive than with most other NDT methods. Another limitation is that internal linear defects oriented parallel to the emitted sound pulse can go undetected as no clear reflection is given. Furthermore, some rough, irregular, inhomogeneous or coarse-grained materials are challenging to properly inspect as a result of poor sound transmission qualities and signal to noise ratios [19].

4.2 PROPOSED MONITORING TECHNOLOGY

Following the currently available technology for CT inspection and monitoring, this section will now present the proposed monitoring technology AE. This method and its application on CT strings, will be the primary focus of the thesis, and will as a result be covered in greater detail than the previous methods.

4.2.1 ACOUSTIC EMISSION

ACOUSTIC EMISSION BASICS

Similar to the cracking sounds made by ice or wood moments before and while collapsing, solid metals release energy in the form of high frequency stress waves as discontinuities are formed due to mechanical loading or stress. With frequencies in the range of 20 – 1000 kHz, above that of audible sound, these stress waves can be detected using high sensitivity transducers [20]. Converting these signals into voltage, amplifying and analyzing these signals form the foundation of AE monitoring. Unlike the other NDT methods described previously, AE monitoring is passive. While the other methods obtain their information by imposing an effect on the monitored material, AE relies solely on the exerted energy from the material itself.

ACOUSTIC EMISSION SOURCES

The exerted energy that forms the basis of the AE process, initiates with stress. Acting in the form of an internal force field in the material, stress distributes externally imposed loadings. Such a force field may be compressive, bending, shearing, tensile or torsion depending on the directional nature of the applied stress. As a response to such a stress field, the material undergoes a change in shape, called strain [21]. Depending on the severity of the stress, the material may deform either elastically meaning temporarily or plastically meaning permanently. The latter involves a change in the relative positioning of atoms, by the sliding of atomic planes creating dislocations. These movements are the underlying mechanism for buckling, yielding, denting etc. [21]. While they do emit some energy in the form of high frequency soundwaves, they are not the primary focus of AE testing.

Breaking and creating new surfaces represents another kind of permanent deformation. Within most steels at a microscopic level, this is most likely to occur on nonmetallic precipitates such as carbide, oxide or sulfide [21]. Larger scale nonmetallic inclusions from the process of rolling or welding the steel are also more likely to break than the metal itself. This is because the metallic matrices are substantially more ductile than the nonmetallic intrusions. However, the breaking of these intrusions is not as influential on the structural integrity of the steel as the breaking of the metal itself, and as a result, the AE from these breakings are not the primary focus of AE testing either.

The primary focus of AE testing is initiation and propagation of cracks within the metal matrices. These cracks produce acoustic signals with higher amplitudes than the previously mentioned occurrences, and is as a result more readily detectable. Furthermore, the amplitude of these waves is dependent on the speed and size of the emitting event. This means that gradually creeping crack event will produce a lower amplitude signal than a rapid, discrete crack event [21]. The typical frequency range of the waves generated by cracks within the metal matrices is from 300 kHz – 1 MHz [21].

In load and hold scenarios, where a load is increased and held then increased and held again, time dependent AE behavior can be observed [21]. Emissions that continue during a constant load hold are generally significant defects that can influence the structural integrity of the test material. During the rise of increasing load however, emissions do not necessarily indicate defects as structurally sound materials also will emit stress waves as the load is increased. For repeated loading scenarios, two distinct effects can be observed. The Kaiser effect is observed in materials that while reloading does not emit acoustic waves before exceeding the primary load level [21]. Specimens that exhibit the Kaiser effect are generally not affected by significant structural flaws at the time of emission. Acoustic emission below the primary load level however, is called the Felicity effect and tends to indicate significant flaws.

While the necessary equipment for AE processing systems can vary in size, they all contain the same elementary components including transducers, filters, preamplifiers and amplifiers [22]. The transducers are essentially the sensors of the system, detecting the small movements of molecules as an AE wave propagates to the surface. These movements are then converted into electrical signals, often by means of a piezoelectric sensor (discussed in section 4.4) [22]. Proper wave transmission between the sensor and the emitting material is ensured by using an acoustic couplant. The couplant is typically some kind of grease that functions by filling out any unevenness between the interface of the material and the sensor. Preamplifiers are used to filter, provide cable drive and gain. They should be placed in close proximity to the transducers, and are in many cases located within the transducer housing [22]. Following the amplifier, a band-pass filter removes frequencies that are not relevant to AE activity by only allowing signals between predefined frequency ranges to pass. This can be around 20 – 1000 kHz. After passing through the filter, the signal enters an analog-digital converter. Equipment used for measurement, storage and display however, can vary in configuration depending on the specific application. Figure 23 illustrates a block diagram of a typical AE system setup with four channels.

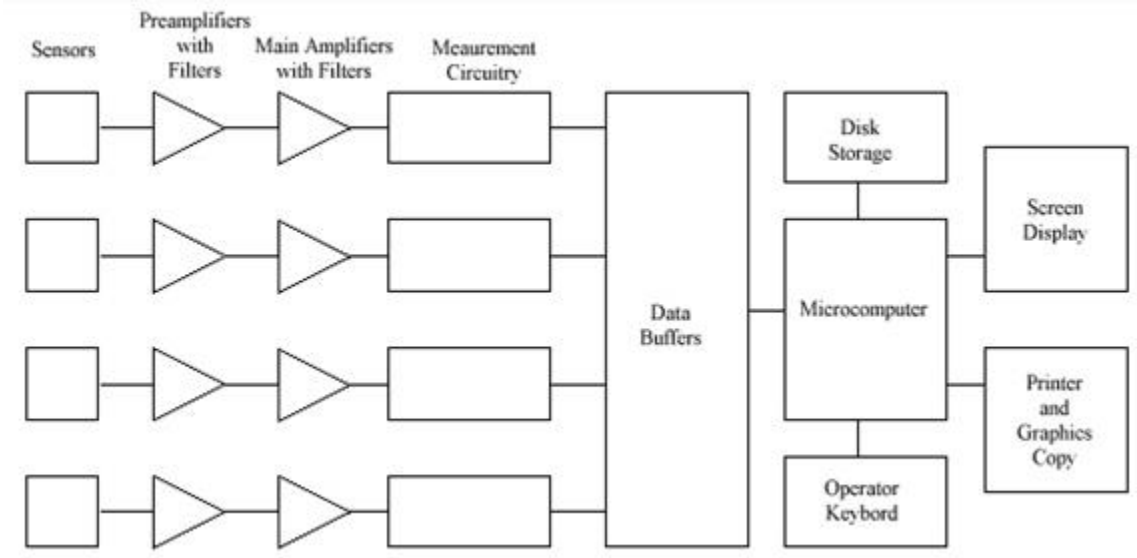

FIGURE 23 – FOUR CHANNEL AE SYSTEM [22]

The AE signals themselves are divided into the three main categories; burst, continuous and mixed mode. Burst type emissions are sudden discrete signals with a near instant rise time and a slightly longer decay time. These signals are generally generated from damage formation in the form of fiber cracking, delamination etc. [23]. Continuous emission signals are often the result of electrical interference or friction acting on the material. The signals appear as multiple bursts overlapping to a degree where they cannot be distinguished or analyzed as individual events. Lastly, mixed mode emission is a combination of bursts and continuous emission. This includes a number of bursts with amplitudes exceeding that of the continuous emission and is the most commonly encountered type of signals. Figure 24 shows the waveform of burst, continuous and mixed mode signals respectively.

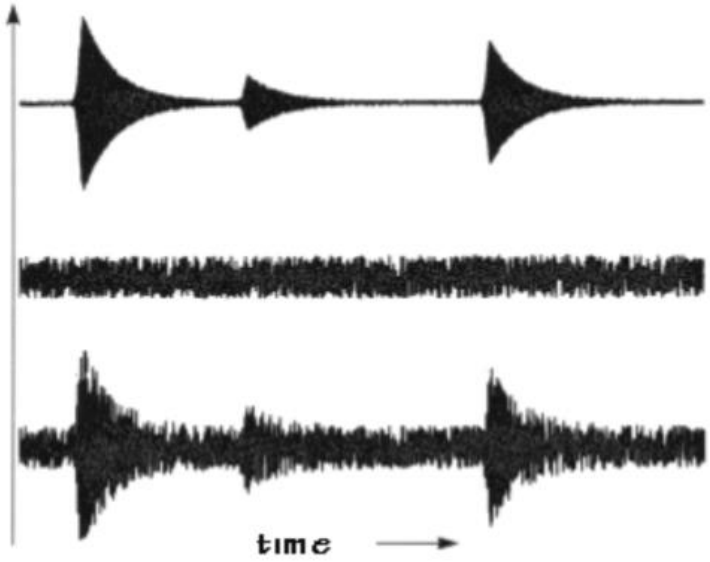

FIGURE 24- BURST, CONTINUOUS AND MIXED MODE SIGNALS [23]

Within the process of collecting the emitted signals, the two concepts hits and events are crucial. "Events" are defined as the physical phenomenon that releases AE signals in a material. A "hit" refers to a single AE signal exceeding a pre-defined voltage threshold and being detected by an electric comparator. Subsequently, the comparator will send a digital pulse signaling the beginning of the "hit" which then initiates the signal measurement process. Continuous oscillation over and under the pre-defined threshold causes the comparator to generate additional signals. Simultaneously several key features of the signal including amplitude, signal energy, duration and counts, are measured using electrical circuits. As the signal energy diminishes to a point where it no longer exceeds the threshold values, the system after a defined amount of time determines that the event has ended.

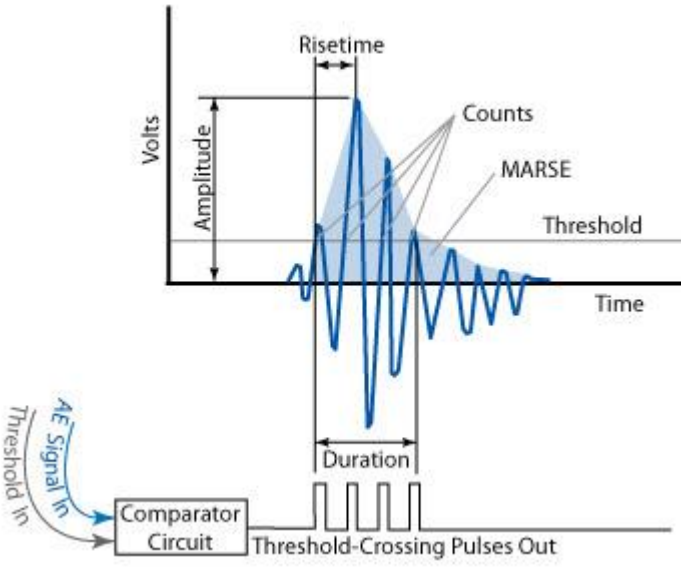

FIGURE 25 -COMMON SIGNAL PARAMETERS EXTRACTED FROM AN AE EVENT [24]

Figure 25, illustrates common parameters that can be extracted from an AE event. Of these parameters, the most important is amplitude, expressed in decibel. This is because the amplitude determines the detectability of the acquired signal and because signals that do not exceed the pre-defined threshold will not be recorded.

The amplitude is calculated from the peak amplitude of the recorded hit and is calculated using the following equation:

$$Decibel = 20 * log_{10}\left(\frac{V}{V_{ref}}\right) - Gain_{Preamplifier}$$

In this equation, the $Gain_{Preamplifier}$ is the gain of the preamplifier which typically is set to 40db. V is the measured voltage with V_{ref} as a reference voltage usually set to (1 µV). Another important parameter is the MARSE, which represents the measured area below the signal envelope. This value can determine the total energy of the recorded emission. Acoustic source localization is possible by using a combination of a known wave velocity, multiple sensors and calculating the arrival time difference between the different sensors. Two sensors allow for a line localization and three sensors can allow for a plane localization.

During analysis of AE signals, the presence of noise can be problematic and can negatively influence the quality of the analysis. Consequently, applying signal de-noising techniques is often required to increase the signal to noise ratio. One such technique aims to extract certain frequencies of the noise by using band pass filters [24]. These filters eliminate the low and or high frequency portions of the signals. While these filters can be effective, caution is advised as noise and information frequencies can overlap in certain situations [24]. Other methods such as short time Fourier transform (STFT) and wavelet transform (WT), decomposes the time dependent AE signals to the frequency domain. Analyzing signals that are decomposed into different scales increases the quality of the analysis significantly. Furthermore, filtering algorithms and thresholding techniques can be applied to de-noise the signals before transforming back to the original domain [24].

4.2.2 LIMITATIONS

The limitations discussed in this section coincide with the limitations listed in ISO 22096 – Acoustic emission, and are described to greater detail in this thesis.

ATTENUATION

Acoustic waves propagating through solid material suffers from decreasing amplitude with increased distance from the source [25]. The phenomenon is known as attenuation and represents a limitation with the applications of AE testing. Figure 10 illustrates the decrease in amplitude with distance. The logarithmic decibel scale referenced to 1µV is used to plot the amplitude on the Y-axis while the X-axis represents distance in feet [21]. As can be seen from Figure 26, the peak amplitude decreases significantly with distance.

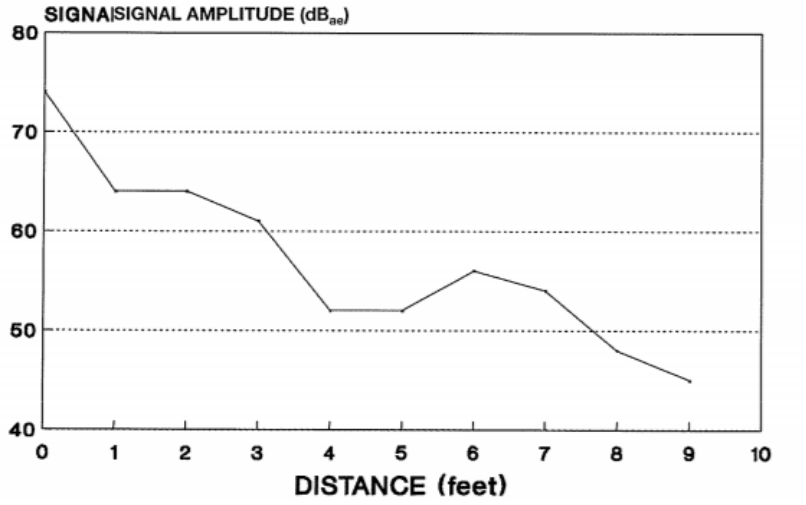

FIGURE 26 - WAVE ATTENUATION [21]

Several factors contribute to the wave attenuation including scattering, absorption and geometric spreading. Over short distances geometric spreading is the most influential factor. Attenuation due to geometric spreading occurs as the waves spread to cover the increasing volume, thus diminishing in intensity. The effect is independent of frequency, but highly impacted by geometry. Boundaries that confine the wave spread reduce the attenuating effect. Consequently, solid rods with a well-defined structure minimize geometric spreading [21].

Over longer distances however, scattering and absorption are the most influential. Scattering occurs at structural boundaries and discontinuities, as parts of the wave energy is reflected. Absorption is the process of kinetic and elastic energy being absorbed by the material it passes through, and ultimately being converted to heat. Non-metallic materials, especially paint and other coatings, tend to absorb more energy than metals [21]. Furthermore, the degree of absorption is increased with higher frequencies as the wavelengths generally are shorter.

NOISE

Any unwanted signals are classified as noise and represent one of the most challenging aspects of AE testing. These signals originate from a variety of acoustic sources. However, friction, electromagnetic interference and impact are the most influential sources. The noise from these sources can interfere with or even overshadow the important signals, thus rendering them useless. Consequently, several approaches to compensating for the noise by means of filtering, transform, blocking or transducer placement must be employed depending on the operating environment [25]. These measures aim to either avoid, protect against or remove the unwanted noise. While these methods can be proficient, they are also time consuming and must be adjusted to each specific application.

OPERATING CONDITIONS

AE technology is heavily reliant on collecting data and performing measurements under similar operating conditions [26]. In continuous monitoring scenarios, this is especially true for the required transducer gain. Variation in operating conditions can cause high amounts of signal variability [26]. Consequently, it can be required to periodically adjust the dynamic range of the AE equipment in order to adapt to the varying operating conditions. For transducers with fixed gain amplification this is not an option. Therefore, transducers with dynamically adjustable should be used for applications with varying operating conditions. On the downside, these are generally more complicated and expensive than the generic COTS fixed gain sensors [26].

4.3 OTHER METHODS

Other viable methods not covered in this thesis include:

Eddy currents, inducing current that travels in loops within the material to be inspected and measuring the magnetic field created by these currents [27].

Penetrant testing, applying a penetrant solution that is pulled into surface defects by capillary forces, cleaning excess solution and inspecting the indication [28].

Visual inspection, detecting defects by direct visual inspection with or without optical aids.

4.4 SUMMARY

TABLE 3 - SUMMARY OF INSPECTION METHODS

Method	Main detection category	Strengths	Limitations
MFL	Material loss and external flaw detection	High degree of automation Does not require coupling with surface	Requires high amount of qualitative analysis Applicable for ferromagnetic materials only
MPI	Surface defects	Rapid inspection of large areas Results are produced directly and at the surface Relatively low equipment cost	Applicable for ferromagnetic materials only Rough surfaces can be problematic Post inspection cleaning and demagnetization
RT	Internal volumetric defects	Applicable for all materials Low surface preparation High level of documentation	Requires skilled operators Can be time consuming HSE hazard with regard to radiation
UT	Internal planar defects	Superior depth of penetration Only requires single sided access Provides defect depth information	Rough surfaces can be problematic Linear / parallel defects can be missed Difficult to inspect thin objects
AE	Internal and external cracks	Passive monitoring Covers large areas Non-intrusive	Susceptible to noise Variable operating conditions can be problematic

5.0 PRACTICAL RESULTS AND ANALYSIS

This section presents the characterized hydraulic noise as well as the acquired results from tensile and fatigue crack testing using ClampOn's reconfigured sand monitoring equipment for acoustic monitoring.

5.1 NOISE CHARACTERIZATION

By studying the recorded AE activity from running the hydraulic test rig, with low loads not generating AE activity from the test specimen, it was possible to identify the noise generated from the rig. As can be seen in Figure 27, which is a screenshot from the monitoring software, the noise appears as a myriad of low energy hits within the range of 18 – 30 dB. Every blue dot in the picture indicates a separate hit, and in the areas where continuous blue lines are formed, it is assumed that

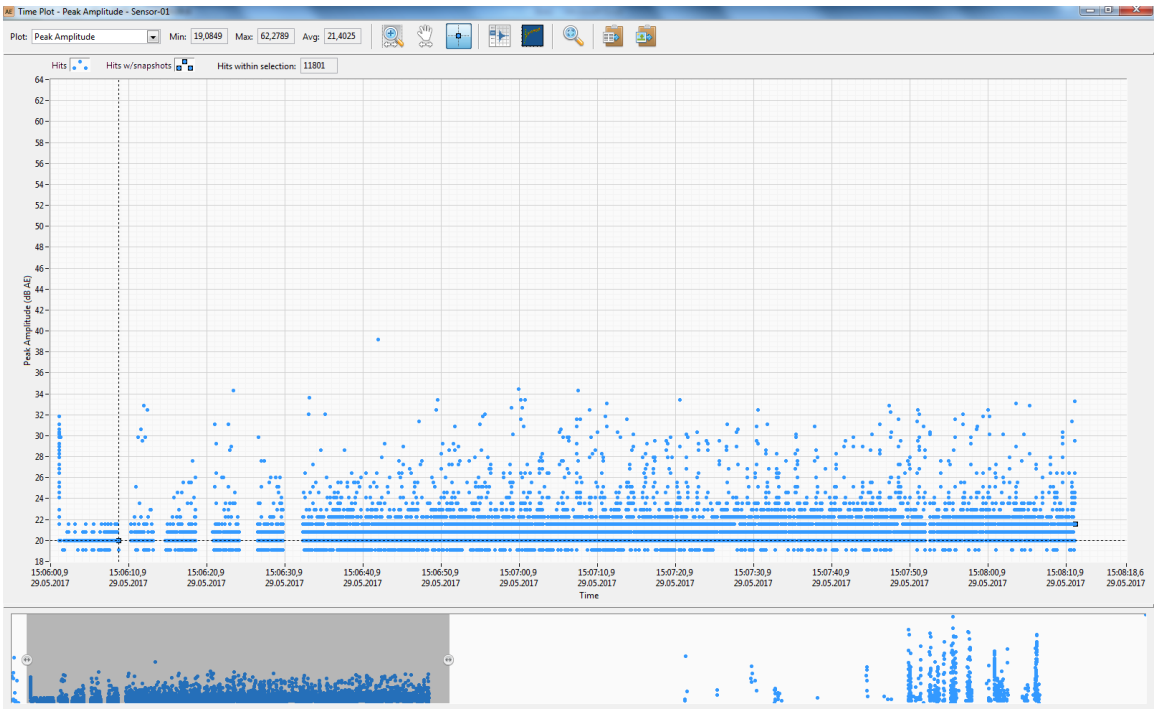

FIGURE 27 – HITS FROM HYDRAULIC NOISE WITHIN THE RANGE OF 18 – 30DB

the sensor becomes saturated. Sensor saturation occurs when the number of hits becomes too high for the sensor to record. As a result, some hits go unrecorded and are not saved in the data file.

Examining the waveform of the hits generated by the hydraulic test rig, reveals that they are continuous rather than the burst type that are seen in the pencil break tests and which are typical for genuine AE hits. Figure 28 is a snapshot showing the waveform of a hydraulic noise signal by plotting the amplitude in µV versus time in µS. Due to the software being an early beta version, it did not offer tools for showing the frequency of the recorded signals. However, zooming in on the signal, counting wave peaks and dividing by the elapsed time gave a very rough estimate of the frequency. For this particular noise signal, the frequency was estimated to about 140 kHz.

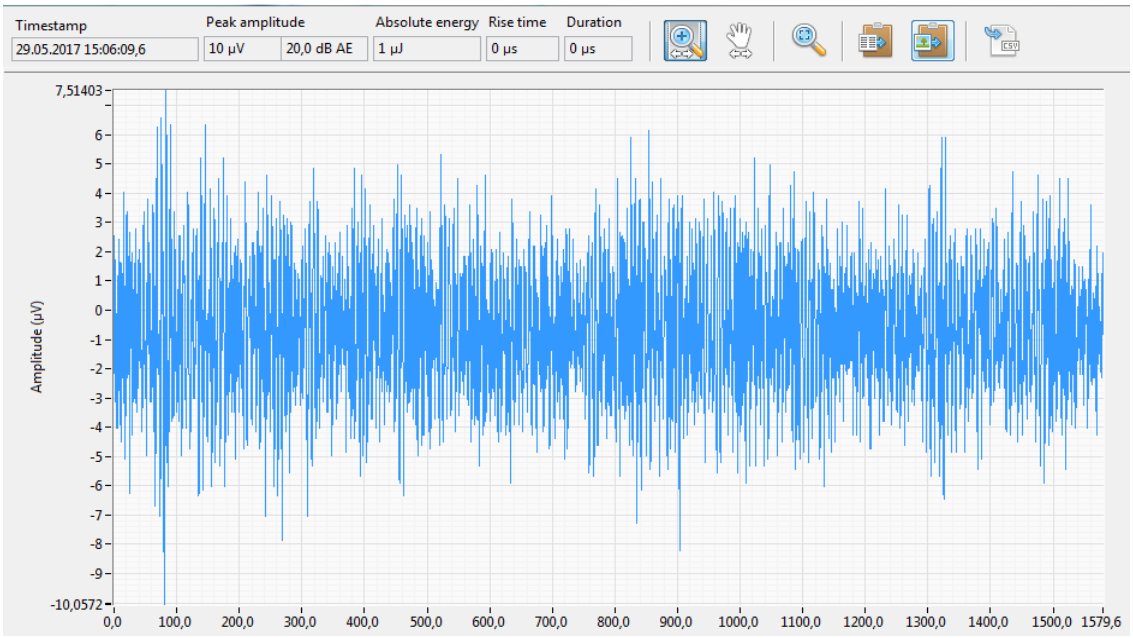

FIGURE 28 - WAVEFORM OF HYDRAULIC NOISE HIT, AMPLITUDE (µV) VS TIME (µS)

5.2 TENSILE TEST

The result for the linear deformation tensile test is presented in this section. As explained in the previous section, the noise generated from the hydraulic test rig completely contaminated the AE recordings in the range from 18 - 30dB. This means that any AE within this range would be impossible to extract without filtering tools, as they would effectively be buried within the noise. Consequently, a threshold value of 30dB was implemented in order to only record hits exceeding 30dB. Figure 29 illustrates the recorded AE activity through the duration of the tensile test. From this test, it was expected to observe AE activity centered around the yield strength, the peak load and the final fracture. However, as can be seen in the figure, there is no activity prior to the final cracking except for one hit which was the result of a pencil break test done to verify that the transducer was working. During the final cracking of the specimen, several hits with amplitudes ranging from 30dB – 65dB can be observed.

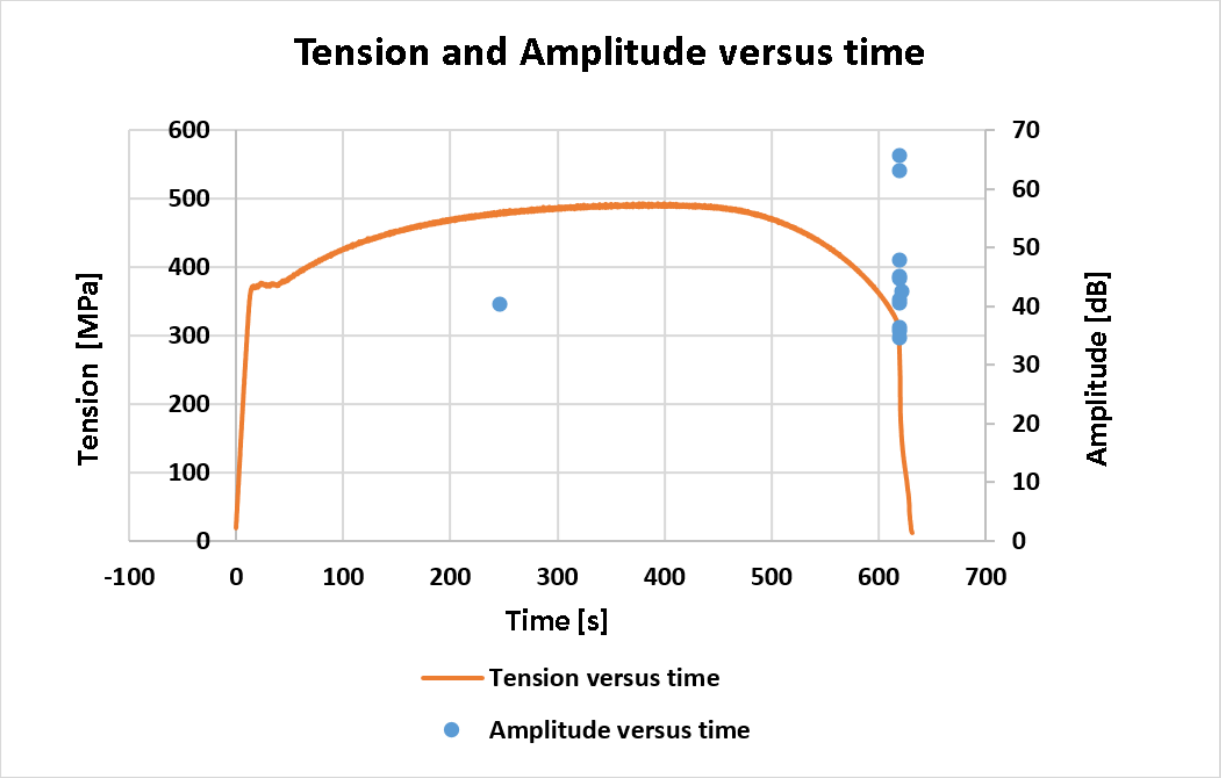

FIGURE 29 - RECORDED AE ACTIVITY DURING TENSILE TEST

5.3 STEPWISE TENSILE TEST

Similar to the linear deformation tensile test, a threshold value of 30dB was set in order to eliminate the hydraulic noise. As previously mentioned, the purpose of this test was to study and verify the Kaiser-effect. Testing by others [29, 30] has shown AE activity and indications of Kaiser-effect at loads as low as 25% of maximum load. However, this test detected no AE activity during the stepwise loading below ultimate load with the set threshold. Like the previous test, the one hit that can be seen in Figure 30 was the result of a pencil break test done during the test process, to verify that the transducer was in fact working properly.

These results indicate that the AE activity, occurring prior to the final breaking of the specimen, has amplitudes not exceeding the threshold value thus effectively being buried within the hydraulic noise. Absent tools for frequency filtering this test was unsuccessful in verifying the Kaiser-effect.

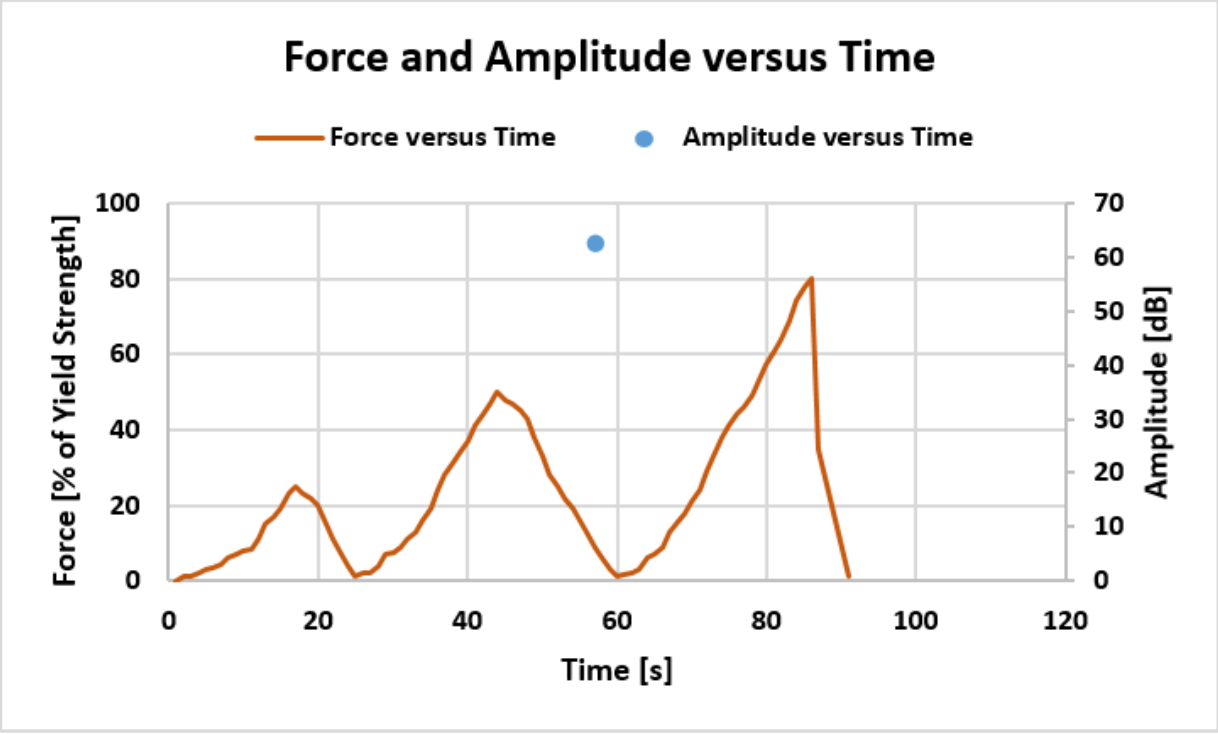

FIGURE 30 - FORCE TIME CURVE FROM STEPWISE TENSILE TEST WITH AE

5.4 FATIGUE TESTS

For the fatigue tests, the amount of recorded AE activity made it necessary to analyze different parameters than individual hits. The tests generated large numbers of hits above the threshold value. In order to get a summarized visualization of the AE activity, and more importantly the change in AE activity, the cumulative energy parameter was selected. With this parameter, constant AE activity generates a linear curve while an increase in AE activity will increase the slope of the curve.

Figure 31 shows the recorded cumulative energy development, in micro joule, of the first test at 50kN with a frequency of 5Hz. From the figure, a steady increase in cumulative energy with some areas of steeper increase can be observed. This development indicates AE activity above threshold level during the entire test period, which is to be expected from a rapid fatigue test. The steep increase early on in the test is thought to either be a result of a possible stress concentration induced by machining the crack in the specimen or extraneous noise related to startup of the hydraulic test rig. Further analysis can be made by studying these AE results in relation to measured crack length development.

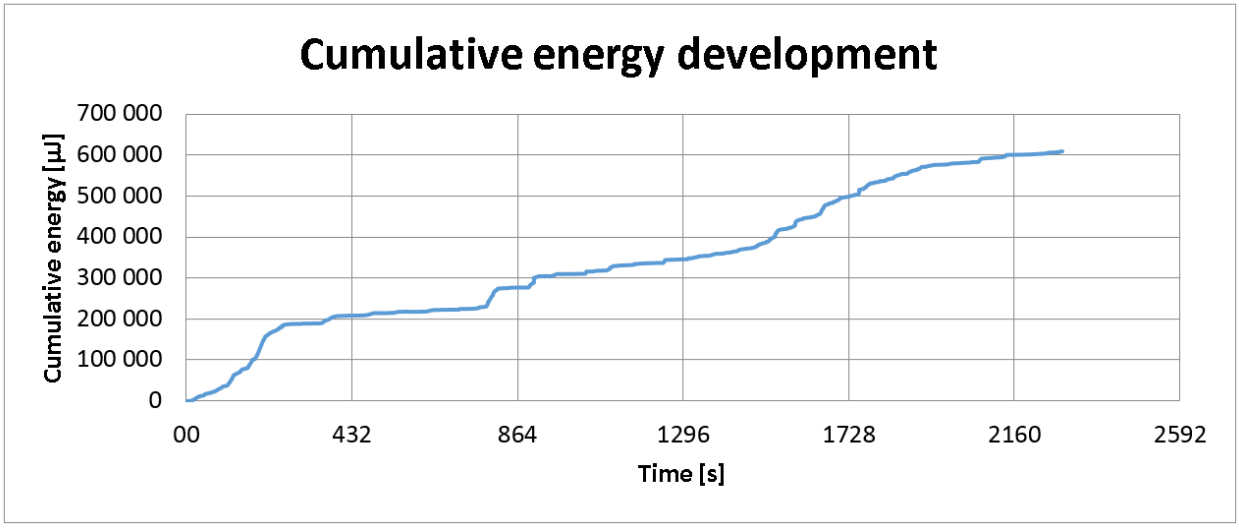

FIGURE 31 - CUMULATIVE ENERGY DEVELOPMENT OF LOW CYCLE FATIGUE TEST (50KN)

In Figure 32, the incremental crack length development of the first fatigue test is plotted versus time giving a visual representation of the crack propagation within the material. From the figure, an exponentially increasing crack length initiating at 500 seconds can be observed. It was decided to plot the crack length versus time as opposed to number of cycles in order to later on study its correlation with data from the AE software, which did not record cycles. However, with a frequency of 5Hz the cycle number can easily be calculated from the time in seconds.

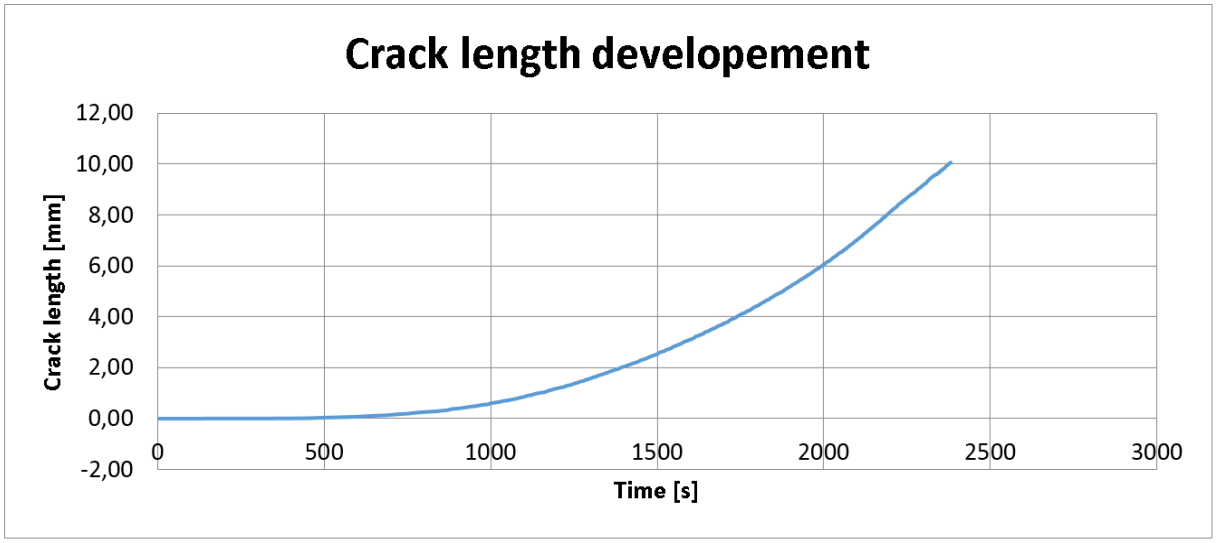

FIGURE 32 - CRACK LENGTH DEVELOPMENT OF LOW CYCLE FATIGUE TEST (50KN)

In Figure 33, the cumulative energy recorded with the AE software is plotted versus the developing crack length.Furthermore, a trendline is added in order to visualize the linear relationship between the two parameters.

By examining the figure, a definite correlation between the two parameters can be observed as the results deviation from the linear trendline is minimal. This observation can be further established by evaluting the coefficient of determination R^2 . This value indicates the proportion of variance between two variables, and can be used as a measure of the regression line's approximation to the actual data. An R^2 value of 1 indicates that the regression line fits the data perfectly. In this case the R^2 is 0,9911, which indicates a very strong fit between the regression line and the recorded data.The definite relationship indicates that the recorded energy is in fact generated from the release of strain energy as the crack propagates in the material. For practical applications, this means that the crack length could be determined directly from the measured cumulative energy.

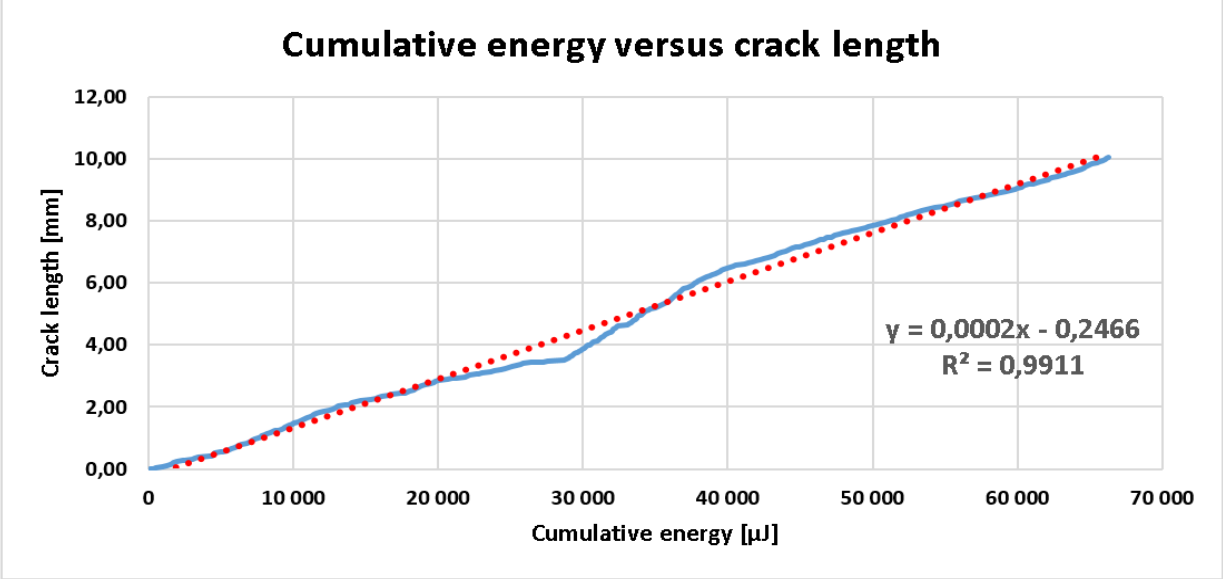

FIGURE 33 - CUMULATIVE ENERGY VERSUS CRACK LENGTH OF LOW CYCLE FATIGUE TEST (50KN)

The second fatigue test was conducted at 35kN and a frequency of 5Hz, resulting in a significantly increased test time. Furthermore, a test specimen without an induced crack was used in order to determine whether the early emissions prior to crack initiation of the previous test were caused by the stress concentrations of the machined crack or from hydraulic startup noise. Figure 34 shows the cumulative energy development of the second fatigue test at 35kN. Similar to the previous test, the cumulative energy is increasing with some areas of steeper increase. Again, emission is initiating prior to crack initiation ultimately indicating that the source of this AE activity is the startup of the hydraulic rig.

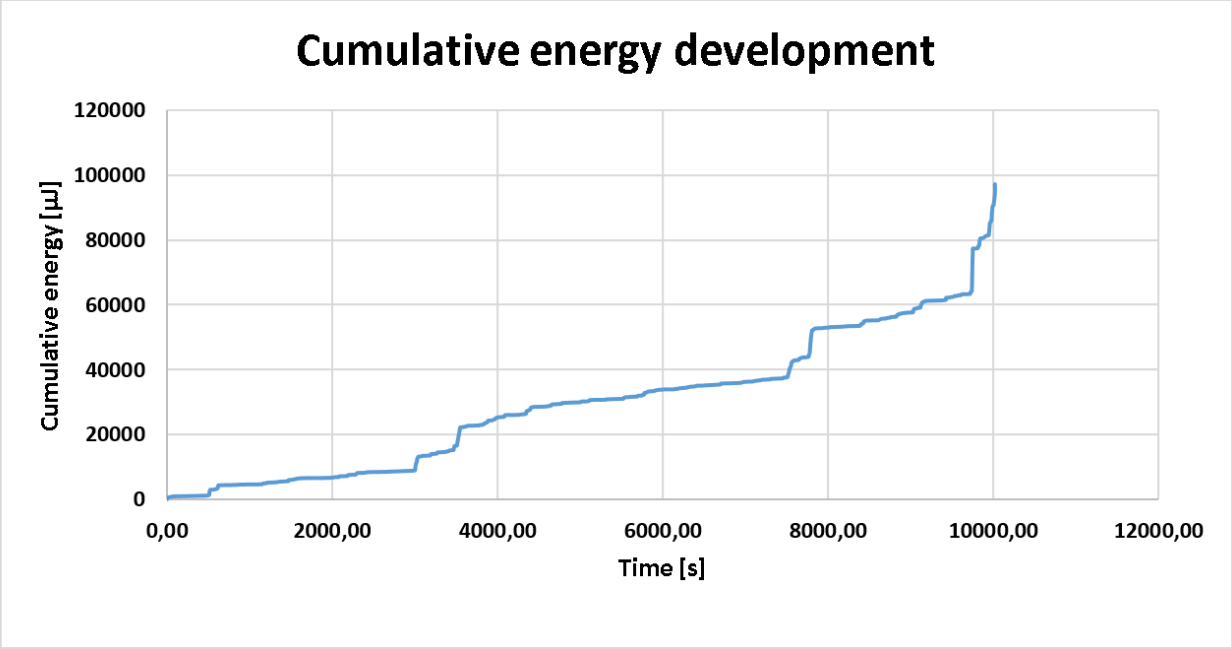

FIGURE 34 - CUMULATIVE ENERGY DEVELOPMENT OF HIGH CYCLE FATIGUE TEST (35KN)

Figure 35 shows an overall similar crack length development to that of the first fatigue test. However, due to the force reduction of the second test, crack initiation does not begin until approximately 5000 seconds. From crack initiation, the crack development is exponential and ends at approximately 14mm.

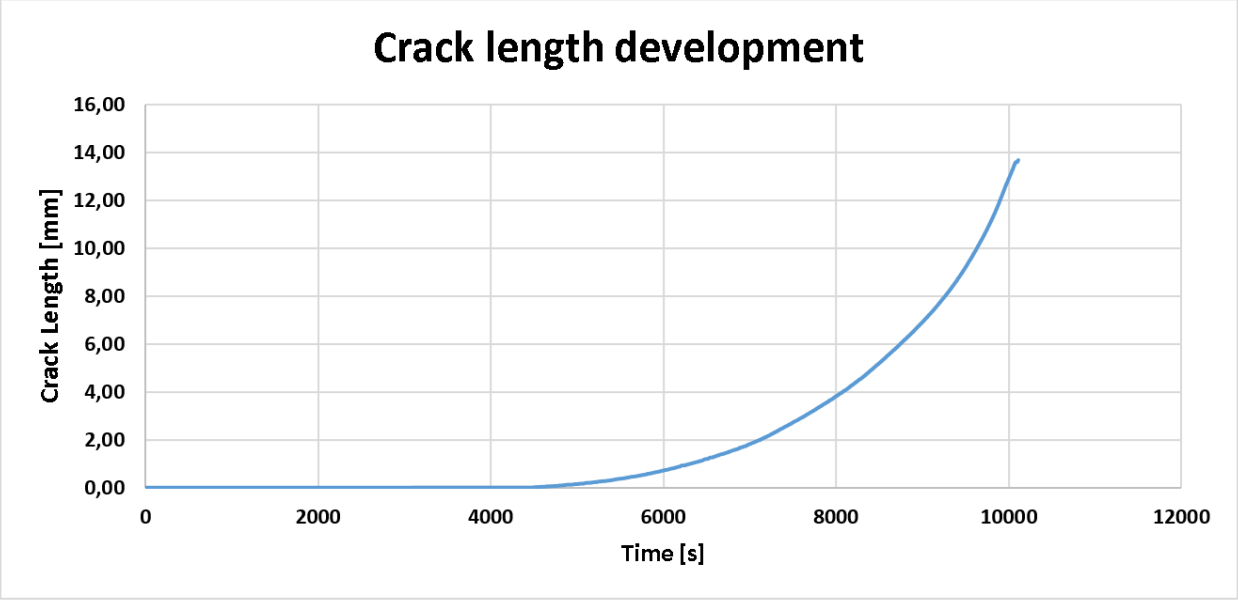

FIGURE 35 - CRACK LENGTH DEVELOPMENT OF HIGH CYCLE FATIGUE TEST (35KN)

Finally, the recorded cumulative energy is again plotted versus the developing crack length in order to study the correlation between the two parameters, as shown in Figure 36. Using a trend line to visualize the linear relationship between the two parameters, a definite correlation can be observed. Furthermore, an R^2 value of 0,9736 indicates a strong fit between the regression line and the recorded data. However, it is recognized that the value is lower than for the previous test. This is believed to be a result of the longer test time allowing for more interference from sources other than genuine AE.

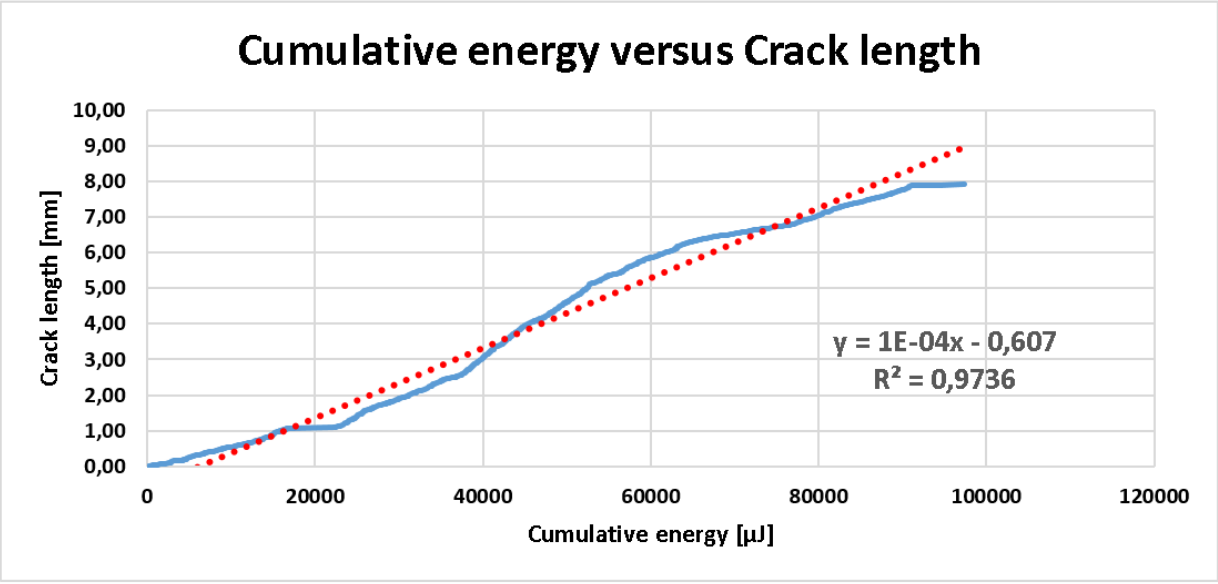

FIGURE 36 - CUMULATIVE ENERGY VERSUS CRACK LENGTH OF HIGH CYCLE FATIGUE TEST (35KN)

6.0 DISCUSSION

First, this section discusses the concept of utilizing AE for condition monitoring of CT by reviewing the potential, proposing a solution and identifying the associated challenges. Then the performed laboratory experiments, their results and possible sources of error are discussed.

6.1 DISCUSSION OF LITTERATURE REVIEW

6.1.1 IDENTIFYING THE POTENTIAL OF AE MONITORING

Paramount in endeavors to change processes or technology is understanding and identifying the potential upsides of the change. Some incentive must exist with regard to economy, safety or environment to rationalize implementing changes. This section aims to illustrate the potential upsides of implementing AE monitoring on CT strings.

Previously in this thesis, the most significant failure modes described in section 3.3 and the most common NDT methods described in section 4 have been presented. From the failure mode section, fatigue cracking is identified as one of the three most influential failure modes. However, from the summary chart of the utilized NDT methods for CT applications, it can be seen that none of the current methods are proficient at detecting the initiation and propagation of fatigue cracks. Other failure modes such as ballooning caused by increased ovality or material loss from corrosion are readily detected by the available NDT methods. This makes it reasonable to assume that introducing a method of detecting fatigue cracking would be beneficial for CT applications. Being able to address the initiating cracks prior to them developing into critical failures is a major contributor to increasing safety. Furthermore, it can allow for a full utilization of the CT string service life, as opposed to relying on fatigue life analysis with design factors. The potential economical upside of this can be significant as long as the costs of performing the condition monitoring are reasonable. In fact, retiring CT strings at 50% of their estimated service life in order to completely avoid failures is not uncommon. This number could possibly be increased to 75% with the proposed monitoring system, while not increasing the risk of catastrophic failure. This could increase CT cost efficiency purely through better equipment utilization.

Early indications of fatigue crack initiation can also result in a reduction both unscheduled and scheduled downtime. This is because it allows for a degree of maintenance planning as opposed to being completely correctional. As a result, the maintenance work can be done more effectively and can be scheduled into maintenance windows with other necessary tasks.

6.1.2 PROPOSED AE MONITORING SOLUTION

Despite AE's ability to monitor across reasonably large distances, the most accurate and reliable results will be achieved by placing the sensing transducer close to the occurring event. Short travel distances reduce the effect of attenuation on the emitted signals (as illustrated by Figure 26) thus increasing the signal to noise ratio. As such, it is important to identify which areas are critical with regard to fatigue cracking during operation. For CT applications, six bending events, at two different locations, occur during one trip. As mentioned in section 3.3, these bending events plastically deform the CT string and are the primary contributors to fatigue cracking. In a standard CT configuration, four of the six bending events occur within the gooseneck, making it the most critical fatigue cracking area. Consequently, the optimal transducer placement would be in the gooseneck, at least from an AE point of view. It is recognized that other practical considerations must be considered, such as vibrations, noise, maintainability and accessibility.

Since the CT string is moving, a conventional static AE transducer will not be applicable. A more suitable solution would be to use one or more rolling AE transducers, possibly placed between the gooseneck rollers. If possible, using a wireless transducer would be beneficial as the placement of the transducer makes it difficult to replace or maintain it. Furthermore, using more than one transducer provides redundancy should one of the sensors fail as well as allowing for defect localization by arrival time difference. Due to the nature of the operating environment, it will be necessary to EX-approve the equipment, possibly by using a protective housing.

AE monitoring will provide valuable information regarding initiation and propagation of fatigue cracks in the CT string. However, it will not monitor other crucial properties such as material loss, ovality and corrosion. Consequently, to ensure complete condition monitoring it will be necessary to combine AE monitoring with one or more other methods. Both MFL and RT, described in section 3, are proficient at detecting volumetric defects and are viable options to combine with AE. MFL however, has the potential for a higher degree of automation than RT making it more suitable for continuous monitoring. A prerequisite for using MFL of course is that the material is ferromagnetic. Should that not be that case, RT is a viable alternative. Combining these two methods with an ovality monitoring method as eddy currents and collecting the information to a single UI would cover the most critical failure modes for CT operations.

6.1.3 Acoustic emission monitoring challenges

The challenges discussed in this section are mostly specific to CT applications, but can also be relevant for other areas of deployment.

Noise and filtering

While extraneous noise within the audible frequency range have little to no effect on AE monitoring with frequency filtering, several sources found in CT applications generate noise that can be problematic while analyzing results [23]. These sources may include; background noise from electronic equipment, aperiodic electro-magnetic interference or AE from mechanisms of no interest. Additionally, AE signals are particularly vulnerable to noise intrusion due to their small amplitudes. Furthermore, variable frequency drives (VFD); often used to control the motor speed in CT drilling, emits electromagnetic radiation with high frequencies that appear as noise bursts for AE equipment. These impulsive bursts are problematic as they couple to AE equipment with frequencies ranging from 10 – 500 kHz thus making them difficult to differentiate from genuine AE hits that range from 300 kHz – 1 MHz [31].

One of the major challenges with AE for condition monitoring purposes relates to eliminating this unwanted interference to ensure accurate conclusions. This is largely because the interference from each application is so different, thus making it difficult to create a single set generic noise reduction and processing method [23]. However, as previously described in section 4.5.1.2, signal conditioning techniques such as filtering and transforms can be effective in increasing the signal to noise ratio in most applications.

SENSOR CALIBRATION AND HARDWARE

Another challenge relates to the existing hardware and the necessary calibration of the hardware. Due to the fact that AE has previously been primarily used for integrity monitoring of structures, their ability to acquire, store and analyze discrete hits is solid [31]. However, for CT monitoring applications continuous and quasi-continuous signals over extended periods have to be captured. This represents a different capture scenario with different hardware demands, which is further convoluted by the need for EX-approving of the equipment. Due to the evolution of AE technology and Moore's law of doubling transistors, it has become possible to continuously monitor AE activity conditions for other than just discrete events. However, the remaining hardware challenge includes developing smart sensors that can relay an understanding of the equipment condition rather than purely streaming raw AE data. This would greatly increase the efficiency of analyzing AE results, as only critical events would be logged and analyzed. In turn, this reduces human intervention and interpretation, thus reducing the risk of human error.

DEFECT CHARACTERIZATION

As mentioned in section 4.5, AE monitoring can allow for defect localization by using several transducers and analyzing the difference in arrival time. However, it is not possible to determine quantitative information such as orientation, depth and size of the defect. This has to be done using a different NDT method, such as UT or RT [25]. Having to rely on another NDT technique can be problematic for several reasons. One of the problems this introduces is that other NDT methods cannot be performed during regular operations. While AE can monitor without intrusion, methods such as RT or UT require operations to be stopped in order to perform inspections.

Furthermore, AE monitoring a requires personnel with qualification and skill that takes time to acquire, something that is also true with other NDT methods such as UT. Training operators to be efficient at both AE and UT is time consuming and expensive.

INDUSTRY SKEPTICISM

For new technology introduced to the oil and gas industry, breaking through the first user barrier can be a significant challenge. This is largely due to the fact that key decision makers in projects and developments tend to avoid using new and unfamiliar technology in order to reduce the associated risk. However, once this barrier has been overcome and the technology has had successful applications, the perceived risk will be lessened. This will in turn make more project leaders willing to select CT with AE monitoring, ultimately establishing the combination as a reliable alternative.

6.2 DISCUSSION OF LABORATORY EXPERIMENTS

As described in the introduction chapter, the purpose of the laboratory experiments was to investigate the suitability of using the ClampOn SandQ monitoring equipment for AE purposes. The results from the conducted testing can be described as mixed, revealing both strengths and weaknesses with the equipment that was used.

6.2.1 TENSILE TESTS

Starting with the linear deformation tensile test, where it was expected to record AE activity within the plastic deformation region and even some within the elastic region. The emissions were expected to be centered around the yield strength, the peak load and the final fracture. The results however, revealed a different scenario as the noise from the hydraulic test rig completely contaminated the lower decibel regions. The presence of this noise was problematic for two reasons, the first was that genuine AE was buried within continuous noise and the second was that the amount of hits caused the sensor to become saturated. Saturating the sensor means that there are too many hits for it to record, thus leaving some hits, which could be genuine AE, unrecorded. As mentioned in both the method and results section, a decibel threshold value was implemented as a measure for eliminating the hydraulic noise. While effective for eliminating the noise, the threshold also eliminated the AE activity within plastic deformation region. Consequently, only AE from the final fracture was captured.

In the view of the author, a better signal to noise ratio could be achieved by applying frequency filtering. This is because the noise from the hydraulic rig is likely to occupy a lower part of the frequency spectrum than the AE from the material. The rough estimate made from enhancing the waveform snapshot of the noise and counting wave peaks resulted in a frequency of 140 kHz. While it is recognized that this method is highly unreliable and inaccurate, it did give an indication of the noise's overall place in the frequency spectrum. As such, high pass filters set to 150 or 200 kHz, or more complex digital filters that could be adjusted to the capturing scenario, would eliminate most if not all the hydraulic noise interference. However, these options were not yet available for the equipment used in these tests.

Much like the linear deformation tensile test, the stepwise tensile test illustrated the same problems. Once again, AE activity prior to final cracking was buried within the hydraulic noise thus not allowing the Kaiser and Felicity effect to be studied. However, it is reasonable to assume that by filtering lower frequencies, the AE data would be revealed and be in agreement with tests performed by others [29, 30].

6.2.2 FATIGUE CRACKING TESTS

More successful results however, were obtained from the fatigue cracking tests. In these tests, the AE activity exceeded the decibel values of the continuous hydraulic noise. Consequently, threshold decibel values could be successfully implemented without eliminating genuine AE activity. Being able to monitor the cumulative energy development in real time also proved to be valuable tool in these tests, as it provided a simple visualization of the recorded AE activity.

From the results, a strong linear relationship between the cumulative AE energy and the crack length could be established in both tests. This relationship was both visualized by using trendlines and quantified through the use of the coefficient of determination R^2. The slight variation in R^2 values between the two tests, is believed to be caused by the increased testing time as possible sources of error have more time to affect the final results.

These results indicate that the equipment is effectively recording the emitted stress energy from crack propagation within the material. Moreover, this relationship suggests a possibility of estimating crack length, to monitor crack development in the material and to predict remaining life of the specimen.

6.2.3 SOURCES OF ERROR

It is the view of the author that some circumstances may have affected the acquired results from the practical experiments. Due to unforeseen technical complications in the process of machining test specimens and rigging the test equipment, the available time for actual testing was limited. Consequently, only a few tests were conducted thus resulting in a small sample size for comparison and analysis. It is recognized that having a larger sample size would strengthen any conclusions drawn from the results.

In addition to this, some technical aspects related to test configuration, may have affected the final results. The primary concern is that false AE activity, from friction caused by relative motion between the sensor and the specimen or even from the opening and closing of the fatigue crack, could be influencing the cumulative energy measurements. Another concern is that inconsistency with the positioning of the glued-on knife edges can cause inaccurate crack opening displacement gauge readings. It seems reasonable to assume that these two sources of error can act as contributing factors to distorting the linear relationship between the cumulative energy and crack length.

7.0 CONCLUSION AND RECOMMENDATIONS FOR FUTURE WORK

The primary objective of this thesis was to investigate the viability of using AE technology as a condition monitoring method to detect the initiation and propagation of cracks in CT.

For the literature review, an introduction to the concept of CT, as well as CT manufacturing, materials, inspection requirements, fatigue life calculation and failure modes was given. This was followed by a review of the available inspection technologies relevant for CT applications. These were described and summarized based on their working principles, advantages and their limitations. Further discussion surrounding the potential, the proposed solution and the associated challenges was then conducted.

From the literature research performed in this thesis, it may be concluded that continuous AE monitoring of CT strings can be a viable solution for predicting fatigue cracking failures. Deployment of this technology may serve to increase the utilization level of CT strings, thus increasing economic viability and safety. However, it was also revealed that AE alone could not provide complete condition monitoring, as the method is unable to monitor properties such as ovality, corrosion and material loss. For this reason, it can also be concluded that AE has to be used in combination with other monitoring techniques in order to obtain complete condition monitoring. MFL and eddy currents were proposed as viable techniques for this purpose.

The secondary objective of this thesis was to test, evaluate and provide recommendations for improving, the equipment's AE monitoring performance.

From the performed tensile and fatigue cracking tests using the reconfigured SandQ transducer for AE monitoring, several conclusions may be drawn. First, from the linear and the stepwise tensile tests it can be concluded that thresholding in scenarios where continuous noise exists with levels exceeding genuine AE activity, is ineffective. In order for the equipment to monitor AE activity within elastic or plastic region, frequency filtering and/or analysis is required.

Second, based on the strong linear relationship that was observed between the increasing crack length and the cumulative energy during the low and high cycle fatigue testing, it can be concluded that the monitoring equipment is capable of detecting, recording and presenting the acoustic emissions generated from crack propagation in low carbon steel. Unlike in the tensile tests, it can be concluded that amplitude thresholding in fatigue cracking tests, where the genuine AE exceeds the hydraulic noise, is greatly effective.

From evaluating the current state of the monitoring equipment provided by ClampOn, it may be concluded that it shows significant promise of becoming a complete and reliable acoustic monitoring system. Most of the fundamental sensing abilities and data visualization tools are in place, and have demonstrated the ability to function in fatigue cracking scenarios. With further development and testing, the system could possibly become applicable for CT applications.

Recommendations for future work primarily involves implementing means for frequency analysis and filtering, be it analogue or digital, and subsequently running several more tensile and fatigue tests. It seems reasonable to expect more successful detection of AE activity within the elastic and plastic region with ClampOn's SandQ equipment if these tools are added. From there it will be beneficial to investigate the possibility of using several sensors simultaneously as guard sensors and for source localization by arrival time analysis. This will make the equipment more reliable by decreasing its susceptibility to extraneous noise, while simultaneously increasing its versatility through the ability of source localization.

8.0 REFERENCES

[1] Macrotrends 2017, *Crude oil price history chart,* Available from: http://www.macrotrends.net/1369/crude-oil-price-history-chart [19 February 2017]

[2] Instron 2017, *8001 Fatigue testing systems*, Available from: http://www.instron.us/en-us/products/testing-systems/dynamic-and-fatigue-systems/servohydraulic-fatigue/8801-floor-model [15 May 2017]

[3] ClampOn 2017, *SandQ monitor,* Available from: http://www.clampon.com/products/topside/sandq-monitor/ [23 February 2017]

[4] Tenaris 2017, *Coiled tubing for onshore and offshore environments,* Available from: http://www.tenaris.com/en/products/coiledtubing.aspx [05 May 2017]

[5] David Bigio et al. 1994, 'Coiled tubing takes center stage', *Oilfield review,* Available from https://www.slb.com/~/media/Files/resources/oilfield_review/ors94/1094/p09_23.pdf [22 February 2017]

[6] Island offshore 2015, *Successful open water coiled tubing drilling,* Available from: http://www.islandoffshore.com/media/news-archive/2014/successful-open-water-coil-tubing-drilling [15 March 2017]

[7] Quality Tubing 2017, *Steel for coiled tubing,* Available from: http://flateurope.arcelormittal.com/updatedec16/section-3.html [15 May 2017]

[8] Miles Ponsonby & Nick McClellan 2002, 'Coiled Tubing in High-Pressure/High-Temperature Wells – Technical Enhancements in the North Sea', *SPE/ICoTA Coiled Tubing Conference and Exhibition,* Available from: https://www.onepetro.org/download/conference-paper/SPE-74819-MS?id=conference-paper%2FSPE-74819-MS [15 March 2017]

[9] API RP 5C7, *Coiled Tubing Operations in Oil and Gas Well Services*, first edition. 2002. Washington, DC: API.

[10] Petro Wiki 2017, 'Coiled tubing', *Society of Petroleum Engineers,* Available from: http://petrowiki.org/Coiled_tubing [10 February 2017]

[11] PetroWiki 2017, 'Coiled tubing fatigue', *Society of Petroleum Engineers,* Available from: http://petrowiki.org/Coiled_tubing_fatigue [22 April 2017]

[12] Van Adrichem, W. P., & Larsen, H. A. 2002, 'Coiled-Tubing Failure Statistics Used to Develop CT Performance Indicators', *Society of Petroleum Engineers,* Available from: https://www.onepetro.org/download/journal-paper/SPE-78808-PA?id=journal-paper%2FSPE-78808-PA [21 February 2017]

[13] International Organization for Standardization 2005, *Design and operation of subsea production systems – Part 7: Completion/Workover riser systems,* ISO 13628-7, Available from: https://www.standard.no/no/Nettbutikk/produktkatalogen/Produktpresentasjon/?ProductID=236899 [17 March 2017]

[14] Chao Zhang et al. 2015, 'Theory and Application of Magnetic Flux Leakage Pipeline Detection', *Multidisciplinary Digital Publishing Institute*, Available from: https://www.ncbi.nlm.nih.gov/pmc/articles/PMC4721765/ [25 February 2017]

[15] NDT Resource Center n.d, *Principles of Magnetic Particle Inspection*, Available from: https://www.nde-ed.org/EducationResources/CommunityCollege/MagParticle/Introduction/basicprinciples.html [11 February 2017]

[16] NDT Resource Center n.d, *Introduction to Radiographic Testing,* Available from: https://www.nde-ed.org/EducationResources/CommunityCollege/Radiography/cc_rad_index.htm [27 April 2017]

[17] Thorsten Achterkirchen, Ph.D. 2014, 'Digital Radiography Goes Mobile for Non-Destructive Testing above the Arctic Circle', *Quality magazine – NDT exclusive,* Available from: http://www.qualitymag.com/articles/91633-digital-radiography-goes-mobile-for-non-destructive-testing-above-the-arctic-circle [27 April 2017]

[18] Kenneth R. Newman & John Lovell 2003, 'A new approach to Ultrasonic Coiled Tubing inspection', *SPE/ICoTA Coiled Tubing Conference and Exhibition,* Available from: https://www.onepetro.org/download/conference-paper/SPE-81722-MS?id=conference-paper%2FSPE-81722-MS [21 April 2017]

[19] NDT Resource Center n.d, *Introduction to Ultrasonic Testing,* Available from: https://www.nde-ed.org/EducationResources/CommunityCollege/Ultrasonics/Introduction/description.html [25 April 2017]

[20] D.G Eitzen & H. N. G. Wadley 1984, 'Acoustic Emission: Establishing the Fundamentals', *National Bureau of Standards,* Vol 89, No. 1 Available from: http://www.virginia.edu/ms/research/wadley/Documents/Publications/Acoustic_Emission_Establishing_Fundamentals.pdf [13 March 2017]

[21] Vrije Universiteit Brussel, *Damage testing, prevention and detection in aeronautics – Acoustic Emission,* Available from: http://mech.vub.ac.be/teaching/info/Damage_testing_prevention_and_detection_in_aeronautics/PDF/acoustic-emission.pdf [21 February 2017]

[22] NDT Resource Center n.d, *Introduction to Acoustic Emission Testing,* Available from: https://www.nde-ed.org/EducationResources/CommunityCollege/Other%20Methods/AE/AE_Equipment.php [13 March 2017]

[23] Rúnar Unnþórsson 2013, 'Hit Detection and Determination in AE Bursts', *InTech,* Available from: http://cdn.intechopen.com/pdfs/43402/InTech-Hit_detection_and_determination_in_ae_bursts.pdf [12 April 2017]

[24] Abida Satour et al. 2013, 'Acoustic emission signal denoising to improve damage analysis in glass fibre-reinforced composites', *Nondestructive Testing and Evaluation,* Vol 29, no 1, Available from: http://www.tandfonline.com/doi/full/10.1080/10589759.2013.854782 [21 March 2017]

[25] NDT Resource Center n.d, *AE Theory – Sources,* Available from: https://www.nde-ed.org/EducationResources/CommunityCollege/Other%20Methods/AE/AE_Theory-Sources.php [02 May 2017]

[26] J. Z. Sikorska & D. Mba 2008, 'Challenges and obstacles in the application of acoustic emission to process machinery', *Proceedings of the institution of Mechanical Engineers, Part E: Journal of Process Mechanical Engineering,* Vol 222, no 1, Available from: http://journals.sagepub.com/doi/pdf/10.1243/09544089JPME111 [04 May 2017]

[27] UniWest 2016, *Principles of Eddy current,* Available from: http://uniwest.com/Principles-of-Eddy-Current-W63.aspx [15 February 2017]

[28] Jim Worman 2011, 'Liquid Penetrant Examination', *The National Board of Boiler and Pressure Vessel Inspectors,* Available from: http://www.nationalboard.org/Index.aspx?pageID=164&ID=374 [14 March 2017]

[29] Uncommon Cries of Cast Iron Elucidated by Acoustic Emission Analysis. Morgner, W and H, Heyse. Chicago: Journal of acoustic emission, 1986, Vol. 5.

[30] Axel Almkvist 2015, *Acoustic emission methods in fatigue testing,* Master thesis, Royal Institute of Technology, Available from: http://www.diva-portal.org/smash/get/diva2:912277/FULLTEXT01.pdf [23 February 2017]

[31] J.Z Sikorska & D. Mba 2006, 'AE Condition Monitoring: Challenges and Opportunities', *Engineering Asset Management*, pp 125-136, Available from: http://rdcu.be/rWor [11 April 2017]